Brain Microstructure Across the Lifespan: Cognitive Links, Network Architecture, and Clinical Implications

Håkon Grydeland

Dissertation for the Degree of PhD

Department of Psychology

Faculty of Social Sciences

University of Oslo

November 2013

Series of dissertations submitted to the
Faculty of Social Sciences, University of Oslo
No. 460

ISSN 1504-3991

Cover: Inger Sandved Anfinsen.
Printed in Norway: AIT Oslo AS.

Produced in co-operation with Akademika publishing, Oslo.
The thesis is produced by Akademika publishing merely in connection with the thesis defence. Kindly direct all inquiries regarding the thesis to the copyright holder or the unit which grants the doctorate.

Contents

1. Acknowledgments

I am definitely standing on the shoulder of giants.

My supervisors Professor Kristine B. Walhovd and Professor Anders M. Fjell have envisioned the projects from which this thesis arose and, supported by grants from the Research Council of Norway, funded the work associated with my degree. I find your generosity, insightful comments, and positivity unique – you inspire me in many facets of life!

Associate Professor Lars T. Westlye has been a highly valued colleague and friend for many years, sharing too generously of his ever-growing expertise, and I am deeply indebted to him. Westlye, Christan K. Tamnes, and Ylva Østby have, with the help of skillful research assistants, collected the majority of the data used in Paper II and III; this contribution to the project can hardly be overstated. Professor Atle Bjørnerud and Paulina Due-Tønnessen at Oslo University Hospital Rikshospitalet also contributed substantially with their imaging expertise during the acquisition of these valuable and high quality data.

I am very grateful to colleagues at the Department of Psychology, Inge Amlien, Astrid Bjørnebekk, Andreas Engvig, Agnete Larsen, Torgeir Moberget and Elin Western to name but a few, for all the help, conversations, and the inspiring work environment they have provided over the years.

Many thanks to Professor Edward T. Bullmore and Petra Vértes, but also to Manuel, Zac, Tun, Mika, Ameera, Catarina, Prantik, Aaron, and Lisa, for making the six months at the Brain Mapping Unit, University of Cambridge, very fruitful and inspiring. This stay was funded by The Department of Psychology, University of Oslo, for which I am very thankful.

Ida Marie Brose, you are truly wonderful – thank you!

2. **List of Papers**

Paper I

Grydeland H, Westlye LT, Walhovd KB, Fjell AM. (2013). Improved Prediction of Alzheimer's Disease with Longitudinal White Matter/Gray Matter Contrast Changes. *Human Brain Mapping*, 34, 2775-2785.

Paper II

Intracortical Myelin Links with Performance Variability Across the Human Lifespan – Results From T1- and T2-weighted MRI Myelin Mapping and Diffusion Tensor Imaging. Grydeland H, Walhovd KB, Tamnes CK, Westlye LT, Fjell AM. (2013). *The Journal of Neuroscience*, 33, 18618-30.

Paper III

Altered Rich Club Organization Across the Human Lifespan – Structural Covariance Networks From T1- and T2-weighted MRI Myelin Mapping
Grydeland H, Bullmore ET, Vértes P, Patel AX, Tamnes CK, Westlye LT, Walhovd KB, Fjell AM.

3. Background

How grasp and predict how humans think, act, and feel? What are the workings of the human psychology, or the mind? And what are the underlying conditions to this mental life? These broad questions overarch the current thesis. Successful problem solving, however, involves breaking a problem down into smaller and putatively more manageable pieces (Sacerdot.Ed, 1974; Duncan, 2013), and these at least centuries-old conundrums afforded no exception. Thus, I aimed at approaching this broad theme by assessing individual differences, change, and network architecture of brain microstructure, and by linking it to behavioral performance on a cognitive task, within the frame of the human lifespan. Using a neuroimaging method sensitive to myelin, my colleagues and I first established the ability to detect change and aid in prediction of diagnostic status, thus showing a potential clinical application. Then, after refining our myelin measure, we delineated intracortical myelin alterations through the lifespan and related it to attentional task performance. Finally, we assessed myelin network structure and discovered how interconnectivity between well-connected core regions differ between children and adolescents, on one hand, and older adults on the other, relative to young adults. The findings provide novel insights into the structural organization of the brain across the lifespan and its relations to cognitive functioning.

3.1 Conceptual Considerations

"Psychology is the Science of Mental Life, both of its phenomena and of their conditions." (James, 1890, p. 15)

A couple of aspects constitute central tenets of the presented works: i) the mind-brain relationship, or the notion that problems regarding the workings of the mind will be informed by studying the structural make-up of the brain by use of neuroimaging. ii) The lifespan framework, and the theoretical and empirical accounts of how a lifespan perspective would offer additional knowledge compared with only assessing parts of the oft-tortuous path from conception to old age. Given their centrality, I will consider them more deeply in turn.

The notion that we can understand the mind, or its constructs that we psychologist call attention, cognitive control, and working memory, to name but a few, by studying the brain constitute a long-standing notion in psychology. In the monumental "The Principles of Psychology" (1890), William James asserts in the opening pages: "The fact that the brain is the one immediate bodily condition of mental operations is indeed so universally admitted nowadays that I need spend no more time in illustrating it, but will simply postulate it and pass on.", before continuing, after a few lines: "Our first conclusion, then, is that a certain amount of brain-physiology must be presupposed or included in Psychology" (James, 1890, page 18). Also today, psychologist would arguably mainly agree with this notion, even though both the dismissal of brain constraining the pattern of thought, and the alternative radical idea that ultimately the science of mental life will be reduced to neural sciences eliminating the tenets of psychology, have been proposed (Changeux and Dehaene, 1989). Still, with the advent of the neuroimaging tools such as magnetic resonance imaging (MRI) used in the current thesis, criticism of naïve reductionism and narrow localizationism of functions to specific brain regions have been put forward (Coltheart, 2006). The aim here is not to undertake this philosophy of science debate, but stress that the work presented here is meant to place itself somewhere at the boarder between cognitive science and neuroscience, aiming to draw upon both approaches. Thus, on one hand, the anchoring of the mind in brain biology implies that the organization of the brain constrain our mental life (Dehaene, 2007). A key rationale for the current work is therefore that functional properties, the mind, to a large extent is determined by the underlying structural architecture (Sporns, 2012), and that a detailed knowledge of this underlying structure would aid us in understanding human cognitive functioning. As Irimia and Horn (2012) points out, such an expectation seems fair given findings that functional specialization can lead to anatomic change, as for instance in the case of trained musicians who feature enlarged sensorimotor, premotor and parietal areas (Schlaug, 2001). On the other hand, even a complete characterization of the structural make-up of the brain will likely not give us answers to all our questions of the mind (Sporns, 2012). Cognitive theory and research are needed to inform brain studies (Mather et al., 2013). Moreover, the criticism of localizationist approach (asking 'where in the brain' questions, instead of 'how') was probably to some extent warranted (Shimamura, 2010). Thus, to understand cognitive abilities like language and memory requires a

shift from mere localization to an analysis of processes and network operations (Treves, 2005; Fuster, 2009). We strive to meet these goals in the present work.

A second central tenet concerns taking a lifespan perspective. What can we gain in knowledge about the brain and cognitive functioning by looking at development through life? Empirically, cognitive performance in general improves from infancy to young adulthood, before it declines with advancing age (Craik and Bialystok, 2006), though with notable exceptions such as vocabulary which show little or no decline, and with great individual variance (Buckner, 2004). In the brain, similar inverted U-shape trajectories have been reported for cortical measures across the lifespan (Sowell et al., 2003). Fascinating studies, however, demonstrate plasticity in both brain and behavior also in later stages of life (Boyke et al., 2008; Engvig et al., 2010). These observations accord with a theoretical framework of lifespan psychology assuming that mechanisms related to maturation, senescence, and learning mutually enrich and constrain each other throughout life, and that it is favorable to understand and study them as interacting forces driving the development of brain and behavior (Shing et al., 2010). Regarding cognitive ability, however, few integrated theoretical accounts exists of lifelong changes (Craik and Bialystok, 2006). Salthouse (1996) proposed a processing-speed account for age-related differences in cognition, focusing on adults: age-related differences in cognition relate to differences in general processing speed of mental operations, which show an inverted-U-shaped trajectory across the lifespan. Craik and Bialystok (2006), however, suggest that lifelong changes depend on changes in abilities of cognitive representation and cognitive control, as well as their interaction. Cognitive control capabilities improve from infancy to young adulthood, before declining, similar to processing speed, but they propose that representational knowledge such as language remains relatively stable in old age. The different trajectories can, however, create similar cognitive outcomes in development and aging by rely more on representation in development, and cognitive control in aging. Thus, even though some abilities show an inverted-U pattern with age across the lifespan, the increase and decline does not necessarily reflect the same underlying processes. The notion that cognitive aging is a mirror-reverse process of development might therefor be too simple, even though some aspects of cognitive change seem to follow the symmetrical pattern of rising and falling over the lifespan. This point is also pertinent for interpreting brain changes. An important task in understanding the mind

and brain is to identify these similarities and pinpoint the differences in. This can be achieved by taking a lifespan perspective (Shing et al., 2010).

3.2 Status of Knowledge

Dehaene (2007), as newly elected chair of Experimental Cognitive Psychology at Collège de France in Paris, concludes "Our good fortune is that we live in a time where the joint advances of psychology and cognitive neuroimaging allow us to begin to make visible, as if the skull were open, the invisible mechanisms of thought" (Dehaene, 2007, page 45). Despite this optimistic view, we are still faced with a daunting task in trying to understand the brain and mind (Devor et al., 2013). We are for one limited in the ability to visualize the brain across the lifespan by ethical considerations and the resolution and neurobiological sensitivity of available imaging techniques. One important underlying neurobiological factor is myelin, the compact membrane sheath covering axons in both gray (GM) and white matter (WM). Myelin is likely crucial for swift and efficient neuronal communication (Zalc and Colman, 2000). Histology studies in humans (Yakovlev and Lecours, 1967) and primates (Feldman and Peters, 1998) have described protracted developmental and aging-related cortical myelin alterations, with myelin changes appearing to be more ubiquitous than for instance loss of neurons (Pakkenberg and Gundersen, 1997; Peters and Sethares, 2002). Although extremely valuable, with its richness in amount of neurobiological detail and specificity, the resource demanding preparation of the *in vitro* specimens limits these and other histology studies' ability to assess large parts of the brain, in a wide age range, while maintaining sufficient representativity across different age cohorts. From a clinical standpoint, it would also be valuable with means to aid valid early diagnostics. Neuroimaging using MRI, however, can answer these calls; conventional T1- and T2-weighted (T1w and T2w, respectively) anatomical MRI facilitates *in vivo* noninvasive characterization of large human samples in a wide age-range with whole-brain coverage. The *in vivo* nature also enables behavioral assessment of cognitive functioning in the same individuals, and for the use in a clinical setting. With automated software suites for analyzing the resulting brain images, various structural and functional brain measures can be relatively easy obtained. However, the MRI methods used in such a large scale lack the

neurobiological specificity of histology. Such MRI-based assessments of cortical integrity as a function of age, and its relations to cognitive abilities have usually been performed using measurements volume or cortical thickness (Bartzokis et al., 2001; Sowell et al., 2003; Gogtay et al., 2004; Fjell et al., 2009; Tamnes et al., 2010; Kochunov et al., 2011; Westlye et al., 2011). For instance, volumes of cortical GM have been shown to increase during childhood, peak in puberty, before declining thereafter (Giedd et al., 1999). Although these morphological measures also probably also reflect changes in myelin (Paus, 2005), these measures are probably suboptimal to assess lifespan changes due to limited neurobiological specificity. This point is potentially important as the neurobiological processes underlying morphological changes might, as mentioned, differ in development and aging (Raz et al., 2005).

In the childhood and adolescents, elimination of synapses (synaptic 'pruning') and myelination have been the most common explanations for the structural imaging findings mentioned above (Paus et al., 2008). Synaptic pruning refers to the process of by which putatively redundant synapses, due to overproduction early in life, are eliminated. Evidence for the hypothesis of pruning as the underlying mechanism comes from post-mortem studies; Huttenlocher and Dabholkar (1997) reported that net synapse elimination occurs late in childhood, ending by age 12 years in auditory cortex, and in midadolescence in prefrontal cortex. However, as noted by Paus et al. (2008), decline in number of synapses probably only affect overall volume to a small degrees according to Bourgeois and Rakic (Bourgeois and Rakic, 1993). Thus, increase in the degree of myelination of intracortical axons seems to be important for the observed morphological effects (Paus, 2005). In aging, myelin has also been implicated in reduction of volume and thickness (Sowell et al., 2003), although other processes such as shrinkage and loss of neurons (Haug et al., 1984), and loss of dendritic arborization (Jacobs et al., 1997) have also been hypothesized to contribute. Still, in both development and aging, the hypothesis of the involvement of myelination stems mostly from histology studies (Yakovlev and Lecours, 1967; Benes, 1989). Thus, there is a need for *in vivo* measurements across the lifespan in large cohorts using imaging methods more sensitive to myelin. Imaging techniques sensitive to microstructure, and particularly myelin, would allow us to infer more precisely regarding the mechanisms underlying brain development and decline.

As mentioned, myelin enables efficient neural communication. Thus, this microstructural feature likely play an important role in brain connectivity (Hagmann et al., 2008). The brain is often said to be a complex network *par excellence* consisting of its myriad of neurons and their connections (Braitenberg and Schüz, 1991). Brain network studies have started to show that the brain have certain characteristic network properties (Bassett and Bullmore, 2009; Bullmore and Sporns, 2009) In particular, several highly connected brain regions, or hubs (Sporns et al., 2007), seem to play an important role in these networks, enabling or at least facilitating efficient global communication (Bullmore and Sporns, 2012; van den Heuvel et al., 2012).

Observations of structural correlations across individuals between different regions, for instance between inferior frontal and superior temporal areas both thought to be involved in language (Lerch et al., 2006), suggest a way to study these connections between regions (Alexander-Bloch et al., 2013a). This phenomenon of structural covariance have been exploited to study both development (Zielinski et al., 2010) and aging (Montembeault et al., 2012), showing increased covariance in certain networks putatively supporting high-order functions such as language in development (peaking in a group aged 12-14 years), and decrease of covariance in the same network in older adults compared with younger adults. However, little is known about the hub structure development in these networks across the lifespan, and particularly their interconnectedness. Moreover, no studies to our knowledge have created covariance networks using a myelin-sensitive measure.

The notion that structural changes across the arch of life discussed above relate to cognition seems warranted. Still, a clear picture of this structure-function relationship is lacking. For instance, Shaw et al. (Shaw et al., 2006) reported associations between cortical maturation and general intellectual abilities in a sample of children and adolescents. However, the relationship differed as a function of intellectual ability level. Specifically, participants with the highest levels of intelligence show a steeper and more prolonged increase in cortical thickness, that is, peaking later, compared with participants with lower intelligence scores. Also in aging, observations of parallel decrease in cognitive functioning and structural integrity as measured by volume or cortical thickness have been made (Raz et al., 2005; Walhovd et al., 2008), but again suggesting non-simple relationships (Walhovd et al., 2004). To better understand how

brain changes link with behavioral performance on cognitive tests, a possibly fruitful approach would be to use measures of cortical integrity with higher neurobiological specificity.

The volume and thickness brain measures discussed above are derived from T1-weighted (T1w) MRI scans. In such scans, the T1-weighted signal intensity reflects the underlying tissue proton relaxation times. Interestingly, several studies have shown that stems mainly from myelin, while cell density and cell properties contribute to a lesser extent (Clark et al., 1992; Barbier et al., 2002; Walters et al., 2003; Eickhoff et al., 2005). Interestingly, instead of using morphometric estimates such as GM volume, it is possible to assess the signal intensity from T1w images directly, usually after some for of normalization to correct for bias inhomogenities in the magnetic field. Several studies, both from our group and others, have indicated that the signal intensity of T1-weighted MRI scans relates to tissue integrity changes as a function of age and clinical group (Davatzikos and Resnick, 2002; Salat et al., 2009; Westlye et al., 2010b). For instance, Salat et al. (2011) observed decreased signal intensity contrast between WM and GM throughout portions of medial and lateral temporal cortex, the precuneus, and the cingulate in Alzheimer's disease (AD) compared to healthy controls. Importantly, Westlye et al. (2010b) demonstrated further how intensity measures enable differentiation of maturation and senescence-related changes by showing how intensity trajectories across the lifespan had an inverted U-shape with peaks in the 20-30s. In contrast, thickness measurements in the same study showed a near-monotonous decrease as a function of age (8-83 years). To summarize, previous studies show that, by using signal intensity derived from T1w MRI scans, more information about underlying neurobiological processes can be obtained. This includes demonstrating intensity differences between patients with AD and healthy controls, and delineating lifespan trajectories. These findings are important foundations in showing that intensity might be a sensitive measure, potentially with clinical applications, yielding more information to the underlying neurobiological process than previous measures of brain integrity across the lifespan. Still, central unresolved questions remain.

The present thesis aims to aid in filling these lacuna in knowledge by assessing myelin structure across the lifespan using two complementary approaches, and test for

cognitive links to intracortical myelin maturation and senescence. To this end, three papers are presented addressing these aims by i) first, validating sensitivity to within-subject change and showing potential clinical applications (Paper I), ii) then, delineating intracortical myelin trajectories through the lifespan, and relating it to behavioral differences in cognitive task performance (Paper II), and iii) showing how myelin structure can inform network topology across the lifespan, and show alterations in a subnetwork putatively important for global brain communication and integration (Paper III).

4. Aims of the Present Studies

As mentioned, studies using T1w signal intensity as a direct measure have indicated that intensity might be a sensitive measure to age-related changes. However, the studies were all cross-sectional, thus not actually testing *change* per se, but age-related differences (see 'Design' below for more information). A further test of whether T1w intensity measures are a sensitive measure detecting change, would therefor be to study the same individual at least twice, preferably over a relatively short time span. Moreover, indications of sensitivity not only to change in itself, but different rates of change between clinical groups, would strongly motivate the further investigations by providing insights into the pathophysiology of clinical conditions and aiding in diagnosis. Morphometric measures aid in correctly classifying brain images in dementia, but there is still need for improved accuracy in the early phase of for instance AD (Frisoni et al., 2010) when the potential for intervention is highest. Could we improve prediction by including intensity measures? No studies have investigated whether tissue contrast changes can be used to distinguish AD patients from controls, and to differentiate subgroups of AD patients. Thus, the main aims of Paper 1 were to validate T1w signal intensity as a measure sensitive to intraindividual change, and to test whether the signal intensity measure could predict from which population a participant was drawn, thus potentially be of aid for diagnosis in clinical settings. To this end, we used a ratio of signal intensity from WM and GM as reported previously. Specifically, we wanted to test whether this WM/GM contrast changes could be used to detect early signs of AD and to predict disease progression beyond what can be

obtained with standard and well-validated morphometric measures of entorhinal cortical thickness and hippocampal volume alone. We employed an automated segmentation procedure (FreeSurfer) to first reconstruct representations of the WM/GM boundary and the pial surface at two different time points (see Methods for more details). Intensity values were sampled from WM and GM tissue at a given distance from the WM/GM boundary, before we calculated WM/GM contrast at each vertex across the surface. The findings demonstrated that T1w signal intensity could indeed detect *changes* and not only age-related differences, and independently aided in predicting group membership.

Taken together with the previous research reviewed above (Westlye et al., 2010b; Salat et al., 2011), the findings in Paper I made us confident and motivated by the fact that T1w intensity detects within-subject changes and improves prediction of dementia. The results therefore paved the way for the studies presented in Papers II and III. Accordingly, we sought to build on our previous research by assessing lifespan trajectories of intracortical integrity and test for cognitive correlates of intensity measures in healthy children, adolescents, and younger and older adults, which had not been reported before. A particularly intriguing prospect for assessing cognitive correlates came from two studies form our group; both found, using diffusion tensor imaging (DTI) characterizing axonal white matter pathways, that intraindividual variability (IIV) on a speeded cognitive control task related to differences in pathway integrity. Whether these effects were limited to longer axonal pathways in the white matter remained unclear; that similar relationship existed in more circumcised intracortical pathways (Ecker et al., 2013) constituted an intriguing hypothesis. Crucially, based on a report showing how increased sensitivity to myelin could be obtained by dividing the T1w signal by a co-registrated T2w image (Glasser and Van Essen, 2011), we now had the opportunity to putatively assess myelin *in vivo* in a large group of individuals across the life span. This T1w/T2w ratio approach allows for assessment *intracortical* myelin, and not, as in Paper I, divide the GM intensity by underlying WM intensity, but instead on the same region in the T2w image. With this refinement, we also wanted to see if we could learn more about intracortical development compared to our previous lifespan intensity study (Westlye et al., 2010b), in addition to test for cognitive associations not previously tested.

The findings from Paper II corroborated previous findings of the intensity being able to differentiate developmental and aging-related trajectories in GM structure, though there were important differences (see Discussion). Importantly, it extended the earlier observations by demonstrating correlations with cognitive measures with a variability measure previously shown to link with white matter pathway integrity. These correlations were predominantly present in the latter part of the lifespan, suggesting structure-age interactions with cognitive functioning. Paper II therefore indicated that T1w/T2w ratio is sensitive to intracortical connectivity and its cognitive correlates.

As discussed above, myelin is crucial for efficient neuronal communication (Zalc and Colman, 2000), and therefore likely contributes importantly to brain network connectivity (Hagmann et al., 2008). As studies have begun to uncover network characteristics of the brain properties (Bassett and Bullmore, 2009; Bullmore and Sporns, 2009), assessing how brain networks might organize based on myelin degree across regions would potentially further illuminate significant principles of brain organization. The results in paper II, showing that the T1w/T2 ratio able to detect age-related differences in intracortical structure putatively related to myelin, and with links to cognition, provided a crucial steppingstone for pursuing the goal of assessing myelin network configurations across the lifespan. We were particularly interested in the hubs, and specifically the increased interconnectedness between these highly connected regions, the so-called 'rich club', which has been reported in white matter pathways networks (van den Heuvel and Sporns, 2011). The rich club has been proposed to be particularly important for global communication and integration (van den Heuvel et al., 2012). The existence of the rich club has not been probed in myelin networks. According, its potential stability across the lifespan remains unknown. Moreover, Paper II showed relative widespread structure-function correlations involving several parts of the brain. To interpret such data, as noted by Duncan (2013) for instance, it is important to consider not just the behavioral correlations with structure in individual regions but also the structural correlations between different regions (Alexander-Bloch et al., 2013a).

5. Methods

5.1 Design

In the present thesis, we used a longitudinal design in Paper I, and a cross-sectional design in Papers II and III. Both designs come with their respective strengths and weaknesses. In a longitudinal design, the same participants are measures repeatedly, in this case twice, and comparisons between measurements are made, allowing for assessments of actual *change* over time. This contrasts with the cross-sectional design, measuring subjects, in this case of various ages across the lifespan, once, and inferring lifespan trajectories based on *age-related differences*, and not actual change. This constitutes a limitation, as there might be various differences between group other than age caused by effects such as health care, nutrition, and environmental toxins differing across the age span tested here. However, also results from longitudinal designs can be hampered by factors such as test-retest effects and selective dropout. Still, the implications cross-sectional studies should be corroborated by longitudinal studies.

5.2 Participants

In Paper I, data from 150 participants were obtained from the well-validated and publicly accessible Open Access Series of Imaging Studies (OASIS, http://www.oasis-brains.org). Recruitment, screening, MRI acquisition details, and previous reports using the current patient population are described and referred to in depth elsewhere (Marcus et al., 2010). Clinical assessment yielded Clinical Dementia Rating (CDR) scores for all participants (Berg, 1988); a global CDR of 0 was taken to indicate absence of dementia, while a CDR of 0.5, 1, and 2 represent very mild, mild, and moderate dementia, respectively. A final sample of 149 participants, 60-96 years of age, all right-handed, was included (for more details, please see tables of sample demographics in all papers).

Participants in Paper II and Paper III were drawn from waves 1 and 2 of 2 longitudinal projects by the Research Group for Lifespan Changes in Brain and Cognition at the University of Oslo, namely 'Neurocognitive Development', and 'Cognition and Plasticity through the Lifespan'. Participants were recruited through newspaper ads, among students and employees at the University of Oslo and from local schools. In

both studies, sub-16 years old participants' parents and participants aged 16 years or older were screened with standardized health interviews to ascertain eligibility; we required participants to be right-handed, fluent Norwegian speakers, and have normal or corrected to normal vision and hearing. Self-reported neurological or psychiatric conditions known to affect normal cerebral functioning, including clinically significant stroke, traumatic brain injury, untreated hypertension, diabetes, use of psychoactive drugs within the last two years, or worries concerning own cognitive status including memory function, were exclusion criteria. All participants above 20 years of age scored < 16 on Beck Depression Inventory (Beck and Steer, 1987) and participants above 40 years of age scored ≥ 26 on Mini Mental State Examination (Folstein et al., 1975).

In Paper II, we included 339 participants, covering continuously the age range from 8.4 to 83.1 years. In Paper III, 259 participants were included, forming 3 age groups covering the lifespan (9-16, 20-40, 60-80 years, respectively). In addition to the health screening, the inclusion of participants for Paper II also depended on the existence of T1w, T2w, and DTI scans of good quality, while in Paper III, the existence of functional scans was a requirement (instead of DTI scans (these functional scans were only available from wave 2 in the youngest participants, while T2w scans were only available from wave 1 in the adults)).

5.3 Cognitive assessment

In Papers II and III, general cognitive abilities were assessed by Wechsler Abbreviated Scale of Intelligence (Wechsler, 1999), and both sampled showed normal range of estimated mean full-scale intelligence quotient (range = 88–145).

In Paper II we use the Eriksen Flanker Task (Eriksen and Eriksen, 1974), a widely behavioral paradigm putatively probing attention and control mechanisms, used to estimate intraindividual variability in performance (MacDonald et al., 2009). This IIV measure reflects performance fluctuations during a single task session (Stuss et al., 2003), and is increased in for instance attention deficit hyperactivity disorder and mild dementia (Hultsch et al., 2000; Castellanos and Tannock, 2002). As in our previous studies (Fjell et al., 2011; Tamnes et al., 2012), we operationalized IIV by calculating

the standard deviation of the RT (sdRT) as the measure of interest, while median RT (mRT) was included as a covariate in all analyses to control for effects of reaction time since a relationship between sdRT and mRT was expected.

5.4 Neuroimaging

To measures structural and functional features of the brain, we employed MRI. Briefly, MRI most commonly exploit the fact that our bodies are composed of ~70% water, or H_20. Each hydrogen component of water contains a proton, which has magnetic properties called *spin* (Huettel et al., 2004). The MRI scanner creates a large static magnet field. When participants scanned in the current project place themselves within this field, the protons of the water molecules align their rotational axis either parallel or anti-parallel to the magnetic field. To measure the magnetic properties of the brain tissue is necessary to transiently apply energy to perturb the protons out of this so-called equilibrium state. To this end, electromagnetic radiation in a specific radio frequency range is applied, changing the relationship between parallel or anti-parallel protons. When the radio frequency is turned off, the protons return to their original state by releasing energy. This release of energy can be measured as an oscillating electromagnetic field by receiver coils above the participant's head. Importantly, the release of energy occurs as a function of the local environment of the protons, such as tissue type, thus enabling differentiation between different types. By repeating this process of transient energy application across space, the spatial origin of the measured signal can be estimated and reconstructed into detailed images.

MRI is a non-invasive method with no known contraindications, and offers great versatility, enabling measurement of various biological aspects of the brain by varying imaging parameters. In the papers included in the thesis, we used 4 types of MRI sequences, namely T1-weighted, T2-weighted, diffusion tensor imaging, and resting-state functional MRI.

All presented work included T1w images, while in we Paper II and III we also included T2w scans to create a T1w/T2w ratio. Both sequences show excellent gray/white contrast. Several studies have combined MRI with histology to assess the source of the signal. Eickhoff et al. (2005) compared T1w and T2w scans with tissue

stained for myelin. They found that intensity profiles extracted from the T1-weighted images and inverted profiles of the T2-weighted images were very similar in shape, and that they reveal similar cortical features. Importantly, the myelin comparison prompted the conclusion that the pattern observed in MR images of the human cerebral cortex originates mainly from its myeloarchitecture with a weaker influence of cell density and cell properties. Similar conclusions have been drawn by Walters et al. (2003) after qualitatively comparing intensity profiles from myelin stains, cell stains, and T1w and T2w images. Finally, direct comparisons of the location and extent of important cortical areas characterized using high-resolution T1w images and myelin-stained sections of the same tissue in marmosets accord closely (Bock et al., 2011). The T1w/T2w ratio approach used in Papers II and III was first presented by (Glasser and Van Essen, 2011). The rationale is that the division of the T1w image by the co-registered T2w image mathematically cancels the signal intensity bias related to the sensitivity profile of the receiver coils, which is highly similar in both images. Importantly, as both imaging types relate to myelin, this ratio approach increase myelin contrast relative to the noise. T1w/T2w ratio maps in humans accord closely to indirect comparisons of myeloarchitectonic maps based on myelin (Glasser and Van Essen, 2011). Thus, although additional validation is required, these findings provide support of the interpretation of T1w/T2w ratio as an estimate of myelin. Still, although T1w and T2w images largely reflect myelin, as mentioned above cell density, and iron (Fukunaga et al., 2010) likely contribute.

Paper II also included diffusion tensor imaging (DTI) to allow for comparisons of the T1w/T2w ratio method with an already established method of microstructure assessment. DTI has emerged as a widely applied and validated method of assessing brain microstructure (Concha et al., 2006). By being sensitive to the diffusion of water molecules, which depends on local microstructure, DTI estimates tissue coherence in each volume element (voxel) in the DTI image. This estimate is derived by fitting a tensor model to the diffusion data yielding three eigenvector and three eigenvalues. We used mean diffusivity as metric, defined as the mean of the three eigenvalues. DTI-derived indices have been linked to myelin (Song et al., 2005), but likely primarily reflect other microstructural properties such as axon fiber diameter and density (Beaulieu, 2002). Consequently, even if not being predominantly a measure of myelin, DTI constitute a viable way of measuring microstructural changes over the

lifespan (Lebel et al., 2012). Although challenges exist in estimating diffusivity in the cortex due to partial-volume effects (Koo et al., 2009), it has been successfully applied to detect GM alterations in for instance aging (Abe et al., 2008).

Finally, in Paper III resting-state functional MRI (rs-fMRI) was used to assess functional connectivity. rs-fMRI has emerged as a powerful tool for investigating functional brain organization after the observation that spontaneous blood oxygen level-dependent activity, an indirect measure of changes in neuronal activity, measured in the left somatosensory cortex correlated with its right homologue and motor areas during rest (Biswal et al., 1995; Fox and Raichle, 2007).

5.5 Cortical Thickness

In all studies, T1w brain images were processed using FreeSurfer involving brain extraction, intensity normalization, automated tissue segmentation, surface-based cortical thickness estimations, generation of white and pial surfaces, surface topology correction, automated whole-brain segmentation, and spherical inter-individual surface alignment (Sled et al., 1998; Dale et al., 1999; Fischl et al., 1999; Fischl and Dale, 2000; Fischl et al., 2002; Fischl et al., 2004a; Fischl et al., 2004b; Segonne et al., 2004). Based on the resulting white matter surface, this is, the surface delineating the border between WM and GM, we sample signal intensity from T1w scans within the cortex. In Paper I, we normalized this value by creating a ratio with the directly subjacent WM values. In contrast, in Papers II and III, following Glasser and Van Essen (2011), we normalized the intracortical T1w values with the corresponding voxel in the co-registered T2w scan form the same subject and session. Following work on T1w signal intensity by Salat et al. (2011) (Paper I), and us (Westlye et al., 2009) and others (Panizzon et al. (2012), we sampled intensity values at a 0.35 fraction into the GM and at a fixed 0.2 distance, in the 2 papers, respectively. An important potential caveat with the presented studies relate to potential effects of sampling distance. For instance, the cortical thickness differences between groups in Paper I could cause more pronounced partial voluming effects in AD when sampling the initial WM and GM signal intensity values, particularly in areas primarily afflicted in AD such as the medial temporal lobes. The mapped intensity values are dependent on the native resolution of the original images, precluding valid inferences on a level

of cortical laminae or axonal architecture even though the surface-based mapping procedure mentioned above used in the present study enables submillimeter morphometric inferences. The validity and comparability of the sampled values therefore depends the contrast gradient at WM/GM boundary and the cortical thickness. As both the contrast and thickness changes with age (Westlye et al., 2009), we cannot be certain that this might confound our results. When controlling for baseline cortical thickness, however, the effect of WM/GM contrast change was still significant. In addition, on visual inspection of both WM and GM signal intensity values from several cases including moderate AD patients, the medial temporal lobe values were similar to other regions not showing WM/GM contrast change differences between groups. This indicate that the GM and WM values were affected by sampling distance from the WM/GM boundary in a similar manner across groups, without any indication of differential contribution of tissue types in AD compared with controls. Further, the similarities of the lifespan trajectories to curves obtained with for instance DTI also suggest that sampling-related issues cause the observed effects. In Paper III, we sampled directly from the WM/GM boundary to potentially reduce such effects, and map values closer to the WM, which has higher levels of myelin.

5.6 Network Construction and Metrics

To construct or model the data as structural networks, we assessed structural covariance (Alexander-Bloch et al., 2013a), that is, the interindividual correlation between brain regions in T1w/T2w ratio. Brain regions were derived using a modified normalized-cut approach yielding approximately equal-sized random parcellations (Craddock et al., 2012). Random parcellations have previously been used to create brain networks (Hagmann et al., 2008; Zalesky et al., 2010). Although this approach does probably not provide functional homogeneity, the random parcellation method used here has been shown to outperformed anatomical atlases and perform nearly as well as the results of functional parcellations in terms of cluster homogeneity and accuracy of representation (Craddock et al., 2012).

Functional connectivity matrices were created by extracting time series of the rs-fMRI scans from the same random parcellations as above. The connectivity, or association, matrices were thresholded to make graph models. In these graphs, the nodes equal the

brain regions included in the graph, and the edges their connections. Sparse networks, with relatively few edges representing relatively strong structural or functional connections, were constructed using a minimum spanning tree approach followed by global thresholding (Alexander-Bloch et al., 2010).

To probe network structure we applied graph theoretical methods (Bassett and Bullmore, 2009; Bullmore and Sporns, 2009). These metrics provide simple yet powerful means to probe network architecture. All the various graph metrics employed have previously been used and validated; please see Paper III for further details.

5.7 Statistics

In Paper I and II, general linear models as employed in the FreeSurfer suite were used to perform statistical tests at each point (vertex) along the cortical surface. In Paper I we also used logistic regression to test for the abilities of the brain measures to aid in discriminating between AD and controls. The logistic regressions were also rerun with a leave-one-out cross-validation scheme to allow for test of prediction ability. Based on the predicted values from the leave-one-out approach, we plotted receiver operating characteristic curves and calculated the area under the curve, as well as sensitivity and specificity using a cutoff value of 0.5.

In Paper II, in order to estimate age-trajectories without any assumption about the form of the curve, we fitted a nonparametric local smoothing model, the smoothing spline, to the mean values of representative regions of interest across the mantle. It has previously been shown that the smoothing spline approach yields less biased solutions than the more commonly employed higher order polynomial functions (Fjell et al., 2010). We used an algorithm that optimizes smoothing level based on a version of Bayesian Information Criterion, which provides a way of obviating the need for arbitrarily chosen smoothing levels.

In Paper III, to test for group differences we used permutation tests given the lack of statistical theory concerning the distribution of most network metrics (Bullmore and Sporns, 2009).

5.8 Ethics

In Paper I, participants participated in accordance with guidelines of the Washington University Human Studies Committee. In Papers II and III, the Regional Committee for Medical and Health Research Ethics approved the studies, and participants under 12 years of age gave oral informed consent, while written informed consent was obtained from all participants from 12 years of age and from a parent or guardian for participants below 18 years of age.

6. Summary Of Papers

Paper 1

Brain morphometry measures derived from magnetic resonance imaging (MRI) are important biomarkers for Alzheimer's disease (AD). The objective of the present study was to test whether we could improve morphometry-based detection and prediction of disease state by use of white matter/ gray matter (WM/GM) signal intensity contrast obtained from conventional MRI scans. We hypothe- sized that including WM/GM contrast change along with measures of atrophy in the entorhinal cortex and the hippocampi would yield better classification of AD patients, and more accurate prediction of early disease progression. T1-weighted MRI scans from two sessions approximately 2 years apart from 78 participants with AD (Clinical Dementia Rating (CDR) = 0.5-2) and 71 age-matched controls were used to calculate annual change rates. Results showed that WM/GM contrast decay was larger in AD compared with controls in the medial temporal lobes. For the discrimination between AD and controls, entorhinal WM/GM contrast decay contributed significantly when included together with decrease in entorhinal cortical thickness and hippocampal volume, and increased the area under the curve to 0.79 compared with 0.75 when using the two morphometric variables only. Independent effects of WM/GM contrast decay and improved classification were also observed for the CDR-based subgroups, including participants converting from either a non-AD status to very mild AD, or from very mild to mild AD. Thus, WM/GM contrast decay increased diagnostic accuracy beyond what was obtained by well-validated morphometric measures alone. The findings suggest that signal intensity properties constitute a sensitive biomarker for cerebral degenration in AD.

Paper II

Cerebral myelin maturation and aging-related degradation constitute fundamental features of human brain integrity and functioning. Although mostly studied in the white matter, the cerebral cortex contains significant amounts of myelinated axons. Still, how intracortical myelin content evolves during development, decays in aging, and links with cognition, remain poorly understood. Several studies have shown the potential of mapping myelin in the cortex by use of T1- (T1w) and T2-weighted (T2w) magnetic resonance imaging signal intensity, which show inverse sensitivity to myelin. Here, we characterized cortical myelin in 339 participants aged 8-83 years by use of a recently introduced T1w/T2w ratio myelin mapping technique and mean diffusivity (MD) from diffusion tensor imaging. To test for cognitive correlates, we employed intraindividual variability (IIV) in performance during a speeded task, a measure recently associated with white matter integrity. The results showed that intracortical myelin maturation was ongoing until the late thirties, followed by 20 relative stable years before declining from the late fifties. For MD, U-shaped paths showing similar patterns were observed, though with less maturational effects in some regions. IIV correlated with both T1w/T2w ratio and MD, mainly indicating that higher degree of intracortical myelin associate with greater performance stability. The relations were more prominent with advancing age, suggesting that aging-related cortical demyelination contributes to increased IIV. The T1w/T2w ratio myelin mapping technique thus seems sensitive to intracortical myelin content in normal development and aging, relates to cognitive functioning, and might constitute an important future tool in mapping normal and clinical brain changes.

Paper III

Myelin supports efficient neural communication and likely contributes importantly to brain connectivity. Integration of information in the brain depends on a set of distributed and highly connected brain regions known as hubs. Studies of white matter pathways suggest that these hubs also demonstrate dense interconnections, forming a so-called 'rich club'. Whether the rich club phenomenon exists in other kinds of structural networks, and, importantly, how the interconnections change through the lifespan, remain unknown. Here, by creating structural covariance networks using a highly myelin-sensitive intensity ratio from T1- and T2-weighted magnetic resonance imaging (MRI), we tested the existence and age-related changes of the rich club in 256 participants forming 3 age groups (9-16, 20-40, and 60-80 years). We also assessed how structurally defined rich club regions participate in the integration of functional communities defined from resting-state functional MRI. We found that myelin networks yielded typical brain network topology including high clustering and modularity. The rich club phenomenon was observed across all age groups involving particularly frontal and parietal regions, but also temporal and occipital regions. Interestingly, the level of rich clubs interconnectedness increased from childhood and adolescents to young adulthood, and declined again in aging, potentially affecting global communication abilities. The rich club regions in the young adults involved a higher number of regions, and were less distributed among functional modules compared with the children and adolescents, potentially signifying that the information transfer workload gets distributed across more hubs from childhood to adulthood. A similar trend was seen in aging. The results indicate that growth and decay of hub interconnectedness through life relates to protracted maturation and early frontal decline of myelin.

7. Discussion

7.1 Myelin Structure Across the Lifespan

7.1.1 Age Trajectories

The unfolding of cortical myelination and demyelination from birth to senium has interested neuroscientists for more than a century (Kaes, 1907). Still, despite the fact that methodological advances in neuroimaging have ignited great interest in macrostructural properties of the cerebral cortex and microstructural properties of WM throughout life, intracortical lifespan changes have to a large extent eluded close examination. In Paper II we characterized degree of intracortical myelin in 339 subjects aged 8-83 years using a new myelin mapping approach (Glasser and Van Essen, 2011). The myelin maps generally demonstrate inverted U-shaped trajectories, indicating a three-staged process of cortical myelin changes: an accelerated myelination process until around 30 years of age, followed by a period of relative stability, before a decrease in myelin content from the late fifties. For comparison, we also delineated DTI-derived mean diffusivity, partly influenced by myelin (Beaulieu, 2002), mapped from the same vertices as the T1w/T2w ratio used for the myelin maps. Also these trajectories generally showed U-shaped patterns, although demonstrating less maturational effects in some regions. The results accord well with the seminal histology study by Yakovlev & Lecours (1967). They reported an increase of myelinated fibers in the association cortices until the third decade and possibly beyond. However, discrepancies with lifespan histology studies assessing restricted regions exist (Lintl and Braak, 1983; Benes et al., 1994). For instance, Benes (1989) reported stable myelination of the cingulate cortices from the second decade. However, the relative sparsity of datapoints in lower or upper age ranges in these studies limits conclusions regarding lifespan trajectories. This highlights the methodological challenges faced by histology studies, while imaging studies facilitate the assessment of a large number of participants. However, even if the current methods are highly sensitive to myelin, we can be less certain about the neurobiological substrate (see below). Thus, future studies combining the two approaches (Concha et al., 2006) would be beneficial.

The T1w/T2w ratio approach refined our previous efforts by using T1w intensity to trace cortical changes in an overlapping sample (Westlye et al., 2010b). Also in Westlye et al., a three-phasic function was delineated, with the greatest age-related decrease observed from the late fifties. Thus, both findings support a three-stages lifespan model reported previously (Jernigan et al., 2001; Raz et al., 2005). However, peaks found in Paper II were estimated to be earlier; for instance, the superior parietal cortex peaked in the middle of the second decade of life. Besides minor processing differences, Westlye et al. (2010b) normalized the T1w signal at each voxel by cerebrospinal fluid signal intensity. The local normalization by the corresponding voxel in the T2w image might render the T1w/T2w method more accurate. However, although the bias field in the T1w and T2w sequences correlate highly, they are not identical (Glasser et al., 2013), which may favor the use of only T1w intensity, either normalized by cerebrospinal fluid, or as a WM/GM ratio like in Paper I. In sum, the findings in Paper II provide novel insights into how the cortex develops across the lifespan, but discrepant results in the precise timing of estimated peaks compared with both histology and imaging studies warrant further corroboration of the results, preferably using a longitudinal approach.

7.1.2 Network Architecture

The main impact of myelin is believed to be in enabling efficient neuronal communication (Zalc and Colman, 2000), but see Braitenberg (1962) as discussed in Glasser, Goyal, Preuss, Raichle, and Van Essen (2013) for a possible central role of myelin in plasticity). Thus, myelin likely plays a vital role in brain connectivity (Hagmann et al., 2008). In Paper II, as discussed above, the intracortical myelin trajectories through life was estimated for individual points (vertices) across the cortical mantle, and the connections between them were not assessed. However, recent studies point to a non-random architectural organization of the brain (Bullmore and Sporns, 2009; Alexander-Bloch et al., 2013b). The main aim of Paper III was therefore to test whether myelin degree in different regions covaried across individuals, thus forming myelin covariance networks, and if the network configuration resembles the organization found in brain networks from other modalities such as rs-fMRI and DTI (Bassett et al., 2009). Specifically, we were particularly interested in testing the existence of high levels interconnectedness between central and well-connected

regions or hubs, the so-called 'rich club' phenomenon (van den Heuvel and Sporns, 2011). Several novel observations were made. First, the results demonstrated the existence of myelin networks with similar properties to previously described brain networks such as increased clustering and modularity compared to random networks. This constituted an important validation of the approach of creating structural covariance networks of the T1w/T2w ratio measure, laying the foundations for subsequent group comparisons. Second, we found evidence of existence of the rich club phenomenon in all 3 groups consisting of children and adolescents, young adults, and older adults, respectively. Finally, when comparing rich club organization, we found that the level of rich club interconnectivity was most pronounced in the young adults, with older adults, and children and adolescents, showing lower levels of interconnections between brain hubs. The study therefore provides new information about structural organization through the lifespan. The results suggest that a feature of development is increased structural interconnectedness between highly connected regions, while aging is characterized by an opposite trend towards less integration between hub brain regions. This difference in interconnectedness might have cognitive correlates (Crossley et al., 2013), and this constitutes a potentially interesting avenue for future research.

Further, quantitative comparisons based on correlations between the rich club structures, that is, which regions indicated to be part or not part of the rich club, confirmed group differences between the youngest and the oldest group relative to the young adults in spatial embedding of rich club regions across the brain. Qualitative inspection suggests that an increased number of frontal regions were involved in the rich club in the young adults. Interestingly, frontal regions show protracted maturation (Gogtay et al., 2004), and an intriguing possibility is that this protracted development also bears on increases in interconnectedness of frontal hubs regions. Still, in Paper II, peak differences between frontal and more posterior regions were not very clear-cut, and this must therefore still be treated as a hypothesis. Also, decrease in structural rich club interconnections frontally might relate to functional brain dynamics; for instance, a posterior-anterior shift in activity is a robust finding in functional imaging aging studies (Davis et al., 2008), that is, increased frontal activity in elderly compared with younger adults. However, the relationship between structural and functional connectivity is probably complex (Damoiseaux and Greicius, 2009; Daselaar et al.,

2013), and future studies studying this coupling across the lifespan would are warranted.

Taken together, these findings provide novel insights suggesting that interconnectedness between well-connected regions relate to myelin and differ through life from childhood and adolescence to young adulthood, and again from young adulthood to older adults. Given that the structural networks was, to our knowledge for the first time, derived by use of a highly myelin sensitive T1w/T2w ratio (Glasser and Van Essen, 2011), age-related alterations in myelin degree seem to be the prime candidate regarding the neurobiological substrate behind the increase and reduction in interconnectedness (Yakovlev and Lecours, 1967).

7.1.3 Clinical Implications

The study of normal variation and healthy cognitive and brain lifespan maturation and senescence may have important clinical implications by making abnormal or atypical patterns of development and aging more readily apparent. Still, an important motivation behind the current work was to more directly assess the ability of signal intensity to detect subtle changes over relative short periods of time (~2 years), and test if such changes could be used to predict group membership related to disease, in this case in older age. Such a finding would point to potential clinical implications. This test was done in Paper I. The main result in Paper I was that changes in WM/GM contrast derived from conventional T1-weighted MRI scans can be used to increase the accuracy of AD diagnosis and prognosis. AD patients and healthy controls differed in the rate of annual WM/GM contrast change especially in the anterior and medial temporal lobe bilaterally. Including WM/GM contrast to logistic regression models together with the well-validated morphometric measures of entorhinal cortical and hippocampal atrophy increased classification accuracy as measured by the area under the curve from 0.75 to 0.79, with a final sensitivity and specificity of 66% and 75%, respectively. Thus, WM/GM contrast changes provided independent and valuable information to diagnostic classification beyond what was obtained by morphometric measures alone. Of note, a significant effect of WM/GM contrast change and an increase in prediction accuracy was also observed for participants in the earliest phases of AD, both very mild AD compared with controls, and a combined group of patients

converting from either a nondementia status to very mild AD, or from very mild to mild AD versus controls. The results suggested that T1w signal intensity changes may also provide a sensitive metric to change related to early pathological processes in AD. However, a larger sample, enabling tests of separate subgroups for conversion from a nondementia status to very mild AD, and from very mild to mild AD versus controls., would have been beneficial for a better understanding of how the results bear on more normal aging. AD likely differs qualitatively from normal cognitive aging (Buckner, 2004), but very mild AD, or mild cognitive impairment (MCI), might be closer to normal aging given an understanding MCI as extreme values on a dimension of normal variation in aging.

The findings corresponded well with cross-sectional findings in the same sample (Salat et al., 2011), although the cross-sectional results showed more widespread effects extending beyond the temporal lobes. This discrepancy likely reflects that cross-sectional data are influenced by accumulated structural changes over longer periods of time, while the longitudinal design in Paper I only will detect ongoing effects when the time intervals is as short as 2 years. Further, an encouraging point regarding the validity of the results regard the region of observed differences. In AD, the characteristic and disease-defining neurofibrillary changes first manifest in the transentorhinal region before proceeding to the neighboring entorhinal region, possibly relating to premature oligendrocyte dysfunction (Braak and Braak, 1991, 1996). The observed differences in WM/GM contrast changes thus concur very well with the anatomical distribution of histopathological events in early phases of AD. The relation between WM/GM contrast, based on T1w intensity, and myelin, further strengthen this observation.

7.2 Functional Links of Myelin Maturation and Senescence

7.2.1 Cognitive Links

We recently related greater within-subject variability (IIV) on a speeded performance task to widespread WM integrity reductions in both development (Tamnes et al., 2012) and (Fjell et al., 2011; Tamnes et al., 2012). However, whether these effects related specifically to the WM fiber pathways connecting distributed brain regions was

unknown. In Paper II we tested this possibility in an overlapping sample, and found that IIV linked to cortical myelin. The effects were independent of general intellectual abilities, suggesting task-specific mechanisms, and right lateralized in line with a greater specialization of the right cortices for visuospatial attention (Mesulam, 1981; Corbetta et al., 1993). Moreover, the findings concurred well with correlations between aging-related myelin defects in the prefrontal cortex and cognitive impairment in primates (Peters and Sethares, 2002). Blackmon et al. (2011) used a ratio of GM and WM T1w intensity and found left-lateralized correlations with verbal working memory performance. We provided novel knowledge by associating cognitive functioning specifically to *cortical* myelin content. Also, we have previously reported cortical thickness-attention correlations in adults overlapping the current sample (Westlye et al., 2011). One may speculate that these effects might be influenced by myelin changes as observed here.

As in our previous WM-IIV studies, the relationship between IIV and intracortical microstructure was strongest in the elderly (≥ 52 years). This observation is interesting as it points to different mechanisms across the lifespan. Van Petten (2004) has assessed several theories of structure-function relationships, specifically between hippocampal volume and memory. As noted by Westlye et al. (2011), this framework may be applied to relationships between other structural and functional measures as well. Her meta-analysis of results from 33 studies led to partial support for a neuropsychological view: that any normal size structure will support normal function, but that loss of tissue in normal aging will lead to a decline. That is, the neuropsychological hypothesis predicts positive correlations between declining structural integrity and concurrent decline in cognitive functioning in older adults, but no relationship or a smaller positive correlation in young adults. As we mainly observed that increased intracortical myelin (higher T1w/T2w ratio or lower MD) related to less variable performance, our findings in accordance with this hypothesis.

However, as a further testament of the complicated structure-function relationship with age noted above, the opposite relationship was found in the young subsample covering posterior regions. The second, ‘developmental’, hypothesis discussed by van Patten predicts negative correlations in children and young adults, as structures such as thickness and GM volume show reduction already from an early age, while the model

proclaims to be agnostic about older adults. This opposite relationship in development as predicted by the maturational hypothesis, could potentially fit our data. As van Petten notes, the maturational hypothesis and the neuropsychological hypothesis are not mutually exclusive. However, we believe the increase in myelin in development observed in Paper II relates to beneficial effects of myelin for improving conduction velocity and timing (Fields, 2008), and thus did not expect this relationship. Moreover, our T1w/T2w ration findings in Paper II fit quite well with our previous findings of lifespan development and cognitive correlates from DTI (Westlye et al., 2010a; Tamnes et al., 2012). Still, the mechanisms underlying age-related alterations on myelin remain poorly understood. A host of processes disrupting myelin have been reported in aging primates, for instance increased thickness of myelin sheaths (Peters et al., 2001) and formation of myelin balloons (Feldman and Peters, 1998). Though putatively being sensitive to myelin, the signal intensity used here does not allow us to discern between these various effects. The same goes for the cognitive processes under investigation, that is, whether the processes are the same (Shing et al., 2010). Taken together, these findings relate to the potentially different effects in maturation and senescence, in keeping with lifespan cognitive theories such as the one proposed by Craik and Bialystor (2006). Future studies should further try and disentangle the observed differences across the lifespan.

7.2.2 Structural-Functional Networks Connections

In Paper III, we did not test for correlations with behavioral performance on cognitive tasks, but we assessed structural-functional relationships by looking at the structural connections of the 'rich club' and the functional community structure, that is, areas of the brain forming functional subnetworks. A central hypothesis concerning the function of the rich club asserts that the rich club serves as a central anatomical infrastructure to interconnect distributed functional regions enabling global communication (van den Heuvel et al., 2012). We found that the connections of the rich club regions in the young adults connected less to different functional modules compared to the youngest and oldest group. The rich club regions in the children-adolescent group also showed tighter connections within the module they were part of as evidenced by a higher within-module z-score. These results do not intuitively fit with the proposed rich club function of integration, and were unexpected. A region

showing high within-module score and high participation coefficient have previously been characterized as a 'connector hub', that is regions well-connected both within their own module and across other modules (Bullmore and Sporns, 2012). Thus, although the core hub nodes were fewer and less interconnected, as evidenced by the rich club results, it seems that, particularly for the children-adolescent group, the nodes taking part in the rich club were more adept at information transfer. One may speculate that this result indicates that information transfer in young adults is more distributed across several regions, reducing the workload for each region and potentially easing information flow. However, we were not able to test the existence of functional community structure differences due to a relative low number of functional scans in the two oldest groups. Such potential differences must be accounted for before clear comparisons can be made, as differences in community structure has previously been reported in development (Fair et al., 2009). Structurally, we only observed a tendency towards higher structural modularity in the young adults compared with the children-adolescent group. As mentioned above, future studies looking into structure-function couplings would be highly beneficial. A particularly interesting topic for future research is the relationship between the rich club and the community structure, and their mutual influence. Interestingly, the fact that the groups show differences in the rich club, but only weaker signs of different community structure, makes one wonder if the interconnections between highly connected nodes, that is, the rich club, might influence the development and decay of modules.

8. Conclusions

Paper I

Decay in contrast ratio between gray and white matter T1-weighted signal intensity increased diagnostic accuracy beyond what was obtained by well-validated morphometric measures alone. The findings suggest that signal intensity properties constitute a sensitive biomarker for cerebral degeneration in Alzheimers' disease, and validate the use of signal intensity for measures of changes in brain microstructure.

Paper II

Intracortical myelin maturation was ongoing until the late thirties, followed by 20 relative stable years before declining from the late fifties, and correlated with a

behavioral measure of intraindividual variability. The relations were more prominent with advancing age, suggesting that aging-related cortical demyelination contributes to increased variability. The myelin mapping based on T1- and T2-weighted imaging therefore seems sensitive to intracortical myelin content in normal development and aging, relates to cognitive functioning, and might constitute an important future tool in mapping normal and clinical brain changes.

Paper III

Structural myelin covariance networks yielded typical brain network topology, and high levels of interconnectedness between well-connected regions – the so-called 'rich club phenomenon' - was observed across all age groups involving particularly frontal and parietal regions, but also temporal and occipital regions. The level of rich clubs interconnectedness increased from childhood and adolescents to young adulthood, and declined again in aging, potentially affecting global communication abilities. The results indicate that growth and decay of hub interconnectedness through the lifespan relates to protracted maturation and early frontal decline of myelin.

9. References

Abe O, Yamasue H, Aoki S, Suga M, Yamada H, Kasai K, Masutani Y, Kato N, Ohtomo K (2008) Aging in the CNS: comparison of gray/white matter volume and diffusion tensor data. Neurobiol Aging 29:102-116.

Alexander-Bloch A, Giedd JN, Bullmore E (2013a) Imaging structural co-variance between human brain regions. Nat Rev Neurosci 14:322-336.

Alexander-Bloch A, Raznahan A, Bullmore E, Giedd J (2013b) The convergence of maturational change and structural covariance in human cortical networks. The Journal of neuroscience : the official journal of the Society for Neuroscience 33:2889-2899.

Alexander-Bloch AF, Gogtay N, Meunier D, Birn R, Clasen L, Lalonde F, Lenroot R, Giedd J, Bullmore ET (2010) Disrupted modularity and local connectivity of brain functional networks in childhood-onset schizophrenia. Front Syst Neurosci 4:147.

Barbier EL, Marrett S, Danek A, Vortmeyer A, van Gelderen P, Duyn J, Bandettini P, Grafman J, Koretsky AP (2002) Imaging cortical anatomy by high-resolution MR at 3.0T: detection of the stripe of Gennari in visual area 17. Magn Reson Med 48:735-738.

Bartzokis G, Beckson M, Lu PH, Nuechterlein KH, Edwards N, Mintz J (2001) Age-related changes in frontal and temporal lobe volumes in men: a magnetic resonance imaging study. Archives of general psychiatry 58:461-465.

Bassett DS, Bullmore ET (2009) Human brain networks in health and disease. Curr Opin Neurol 22:340-347.

Bassett DS, Bullmore ET, Meyer-Lindenberg A, Apud JA, Weinberger DR, Coppola R (2009) Cognitive fitness of cost-efficient brain functional networks. Proc Natl Acad Sci U S A 106:11747-11752.

Beaulieu C (2002) The basis of anisotropic water diffusion in the nervous system - a technical review. NMR Biomed 15:435-455.

Benes FM (1989) Myelination of cortical-hippocampal relays during late adolescence. Schizophr Bull 15:585-593.

Benes FM, Turtle M, Khan Y, Farol P (1994) Myelination of a key relay zone in the hippocampal formation occurs in the human brain during childhood, adolescence, and adulthood. Archives of general psychiatry 51:477-484.

Berg L (1988) Clinical Dementia Rating (CDR). Psychopharmacol Bull 24:637-639.

Biswal B, Yetkin FZ, Haughton VM, Hyde JS (1995) Functional connectivity in the motor cortex of resting human brain using echo-planar MRI. Magn Reson Med 34:537-541.

Blackmon K, Halgren E, Barr WB, Carlson C, Devinsky O, DuBois J, Quinn BT, French J, Kuzniecky R, Thesen T (2011) Individual differences in verbal abilities associated with regional blurring of the left gray and white matter boundary. The Journal of neuroscience : the official journal of the Society for Neuroscience 31:15257-15263.

Bourgeois JP, Rakic P (1993) Changes of synaptic density in the primary visual cortex of the macaque monkey from fetal to adult stage. The Journal of neuroscience : the official journal of the Society for Neuroscience 13:2801-2820.

Boyke J, Driemeyer J, Gaser C, Buchel C, May A (2008) Training-induced brain structure changes in the elderly. The Journal of neuroscience : the official journal of the Society for Neuroscience 28:7031-7035.

Braitenberg V (1962) A note on myeloarchitectonics. J Comp Neurol 118:141-156.

Braitenberg V, Schüz A (1991) Anatomy of the cortex : statistics and geometry. Berlin: Springer-Verlag.

Braak H, Braak E (1991) Demonstration of amyloid deposits and neurofibrillary changes in whole brain sections. Brain Pathol 1:213-216.

Braak H, Braak E (1996) Development of Alzheimer-related neurofibrillary changes in the neocortex inversely recapitulates cortical myelogenesis. Acta Neuropathol 92:197-201.

Buckner RL (2004) Memory and executive function in aging and AD: multiple factors that cause decline and reserve factors that compensate. Neuron 44:195-208.

Bullmore E, Sporns O (2009) Complex brain networks: graph theoretical analysis of structural and functional systems. Nat Rev Neurosci 10:186-198.

Bullmore E, Sporns O (2012) The economy of brain network organization. Nat Rev Neurosci 13:336-349.

Castellanos FX, Tannock R (2002) Neuroscience of attention-deficit/hyperactivity disorder: the search for endophenotypes. Nat Rev Neurosci 3:617-628.

Changeux JP, Dehaene S (1989) Neuronal models of cognitive functions. Cognition 33:63-109.

Clark VP, Courchesne E, Grafe M (1992) In vivo myeloarchitectonic analysis of human striate and extrastriate cortex using magnetic resonance imaging. Cereb Cortex 2:417-424.

Coltheart M (2006) What has functional neuroimaging told us about the mind (so far)? Cortex 42:323-331.

Concha L, Gross DW, Wheatley BM, Beaulieu C (2006) Diffusion tensor imaging of time-dependent axonal and myelin degradation after corpus callosotomy in epilepsy patients. Neuroimage 32:1090-1099.

Corbetta M, Miezin FM, Shulman GL, Petersen SE (1993) A PET study of visuospatial attention. The Journal of neuroscience : the official journal of the Society for Neuroscience 13:1202-1226.

Craddock RC, James GA, Holtzheimer PE, 3rd, Hu XP, Mayberg HS (2012) A whole brain fMRI atlas generated via spatially constrained spectral clustering. Human brain mapping 33:1914-1928.

Craik FI, Bialystok E (2006) Cognition through the lifespan: mechanisms of change. Trends Cogn Sci 10:131-138.

Crossley NA, Mechelli A, Vertes PE, Winton-Brown TT, Patel AX, Ginestet CE, McGuire P, Bullmore ET (2013) Cognitive relevance of the community structure of the human brain functional coactivation network. Proc Natl Acad Sci U S A 110:11583-11588.

Dale AM, Fischl B, Sereno MI (1999) Cortical surface-based analysis. I. Segmentation and surface reconstruction. Neuroimage 9:179-194.

Damoiseaux JS, Greicius MD (2009) Greater than the sum of its parts: a review of studies combining structural connectivity and resting-state functional connectivity. Brain Struct Funct 213:525-533.

Daselaar SM, Iyengar V, Davis SW, Eklund K, Hayes SM, Cabeza RE (2013) Less Wiring, More Firing: Low-Performing Older Adults Compensate for Impaired White Matter with Greater Neural Activity. Cerebral cortex.

Davatzikos C, Resnick SM (2002) Degenerative age changes in white matter connectivity visualized in vivo using magnetic resonance imaging. Cereb Cortex 12:767-771.

Davis SW, Dennis NA, Daselaar SM, Fleck MS, Cabeza R (2008) Que PASA? The posterior-anterior shift in aging. Cerebral cortex 18:1201-1209.

Dehaene S (2007) A Few Steps Toward a Science of Mental Life. Mind Brain Educ 1:28-47.

Devor A et al. (2013) The challenge of connecting the dots in the B.R.a.I.N. Neuron 80:270-274.

Duncan J (2013) The structure of cognition: attentional episodes in mind and brain. Neuron 80:35-50.

Ecker C, Ronan L, Feng Y, Daly E, Murphy C, Ginestet CE, Brammer M, Fletcher PC, Bullmore ET, Suckling J, Baron-Cohen S, Williams S, Loth E, Murphy DG (2013) Intrinsic gray-matter connectivity of the brain in adults with autism spectrum disorder. Proc Natl Acad Sci U S A 110:13222-13227.

Eickhoff S, Walters NB, Schleicher A, Kril J, Egan GF, Zilles K, Watson JD, Amunts K (2005) High-resolution MRI reflects myeloarchitecture and cytoarchitecture of human cerebral cortex. Hum Brain Mapp 24:206-215.

Engvig A, Fjell AM, Westlye LT, Moberget T, Sundseth O, Larsen VA, Walhovd KB (2010) Effects of memory training on cortical thickness in the elderly. Neuroimage 52:1667-1676.

Eriksen BA, Eriksen CW (1974) Effects of noise letters upon the identification of a target letter in a nonsearch task. Percept Psychophys 16:143–149.

Feldman ML, Peters A (1998) Ballooning of myelin sheaths in normally aged macaques. J Neurocytol 27:605-614.

Fields RD (2008) White matter in learning, cognition and psychiatric disorders. Trends Neurosci 31:361-370.

Fischl B, Dale AM (2000) Measuring the thickness of the human cerebral cortex from magnetic resonance images. Proc Natl Acad Sci U S A 97:11050-11055.

Fischl B, Sereno MI, Dale AM (1999) Cortical surface-based analysis. II: Inflation, flattening, and a surface-based coordinate system. Neuroimage 9:195-207.

Fischl B, Salat DH, van der Kouwe AJ, Makris N, Segonne F, Quinn BT, Dale AM (2004a) Sequence-independent segmentation of magnetic resonance images. Neuroimage 23 Suppl 1:S69-84.

Fischl B, Salat DH, Busa E, Albert M, Dieterich M, Haselgrove C, van der Kouwe A, Killiany R, Kennedy D, Klaveness S, Montillo A, Makris N, Rosen B, Dale

AM (2002) Whole brain segmentation: automated labeling of neuroanatomical structures in the human brain. Neuron 33:341-355.

Fischl B, van der Kouwe A, Destrieux C, Halgren E, Segonne F, Salat DH, Busa E, Seidman LJ, Goldstein J, Kennedy D, Caviness V, Makris N, Rosen B, Dale AM (2004b) Automatically parcellating the human cerebral cortex. Cereb Cortex 14:11-22.

Fjell AM, Westlye LT, Amlien IK, Walhovd KB (2011) Reduced white matter integrity is related to cognitive instability. The Journal of neuroscience : the official journal of the Society for Neuroscience 31:18060-18072.

Fjell AM, Walhovd KB, Westlye LT, Ostby Y, Tamnes CK, Jernigan TL, Gamst A, Dale AM (2010) When does brain aging accelerate? Dangers of quadratic fits in cross-sectional studies. Neuroimage 50:1376-1383.

Fjell AM, Westlye LT, Amlien I, Espeseth T, Reinvang I, Raz N, Agartz I, Salat DH, Greve DN, Fischl B, Dale AM, Walhovd KB (2009) High Consistency of Regional Cortical Thinning in Aging across Multiple Samples. Cereb Cortex.

Fox MD, Raichle ME (2007) Spontaneous fluctuations in brain activity observed with functional magnetic resonance imaging. Nat Rev Neurosci 8:700-711.

Frisoni GB, Fox NC, Jack CR, Jr., Scheltens P, Thompson PM (2010) The clinical use of structural MRI in Alzheimer disease. Nat Rev Neurol 6:67-77.

Fukunaga M, Li TQ, van Gelderen P, de Zwart JA, Shmueli K, Yao B, Lee J, Maric D, Aronova MA, Zhang G, Leapman RD, Schenck JF, Merkle H, Duyn JH (2010) Layer-specific variation of iron content in cerebral cortex as a source of MRI contrast. Proc Natl Acad Sci U S A 107:3834-3839.

Fuster JM (2009) Cortex and memory: emergence of a new paradigm. J Cogn Neurosci 21:2047-2072.

Giedd JN, Blumenthal J, Jeffries NO, Castellanos FX, Liu H, Zijdenbos A, Paus T, Evans AC, Rapoport JL (1999) Brain development during childhood and adolescence: a longitudinal MRI study. Nat Neurosci 2:861-863.

Glasser MF, Van Essen DC (2011) Mapping human cortical areas in vivo based on myelin content as revealed by T1- and T2-weighted MRI. J Neurosci 31:11597-11616.

Glasser MF, Goyal MS, Preuss TM, Raichle ME, Van Essen DC (2013) Trends and properties of human cerebral cortex: Correlations with cortical myelin content. Neuroimage.

Gogtay N, Giedd JN, Lusk L, Hayashi KM, Greenstein D, Vaituzis AC, Nugent TF, 3rd, Herman DH, Clasen LS, Toga AW, Rapoport JL, Thompson PM (2004) Dynamic mapping of human cortical development during childhood through early adulthood. Proc Natl Acad Sci U S A 101:8174-8179.

Hagmann P, Cammoun L, Gigandet X, Meuli R, Honey CJ, Wedeen VJ, Sporns O (2008) Mapping the structural core of human cerebral cortex. PLoS Biol 6:e159.

Haug H, Kuhl S, Mecke E, Sass NL, Wasner K (1984) The significance of morphometric procedures in the investigation of age changes in cytoarchitectonic structures of human brain. Journal für Hirnforschung 25:353-374.

Huettel SA, Song AW, McCarthy G (2004) Functional Magnetic Resonance Imaging. Sunderland, MA: Sinauer Associates.

Hultsch DF, MacDonald SW, Hunter MA, Levy-Bencheton J, Strauss E (2000) Intraindividual variability in cognitive performance in older adults: comparison of adults with mild dementia, adults with arthritis, and healthy adults. Neuropsychology 14:588-598.

Huttenlocher PR, Dabholkar AS (1997) Regional differences in synaptogenesis in human cerebral cortex. J Comp Neurol 387:167-178.

Irimia A, Van Horn JD (2012) The structural, connectomic and network covariance of the human brain. Neuroimage 66C:489-499.

Jacobs B, Driscoll L, Schall M (1997) Life-span dendritic and spine changes in areas 10 and 18 of human cortex: a quantitative Golgi study. J Comp Neurol 386:661-680.

James W (1890) The Principles of Psychology. New York: Holt.

Jernigan TL, Archibald SL, Fennema-Notestine C, Gamst AC, Stout JC, Bonner J, Hesselink JR (2001) Effects of age on tissues and regions of the cerebrum and cerebellum. Neurobiol Aging 22:581-594.

Kaes T (1907) Die Grosshirnrinde des Menschen in ihren Massen und in ihrem Fasergehalt. Jena: Fischer.

Kochunov P, Glahn DC, Lancaster J, Thompson PM, Kochunov V, Rogers B, Fox P, Blangero J, Williamson DE (2011) Fractional anisotropy of cerebral white matter and thickness of cortical gray matter across the lifespan. Neuroimage 58:41-49.

Koo BB, Hua N, Choi CH, Ronen I, Lee JM, Kim DS (2009) A framework to analyze partial volume effect on gray matter mean diffusivity measurements. Neuroimage 44:136-144.

Lebel C, Gee M, Camicioli R, Wieler M, Martin W, Beaulieu C (2012) Diffusion tensor imaging of white matter tract evolution over the lifespan. Neuroimage 60:340-352.

Lerch JP, Worsley K, Shaw WP, Greenstein DK, Lenroot RK, Giedd J, Evans AC (2006) Mapping anatomical correlations across cerebral cortex (MACACC) using cortical thickness from MRI. Neuroimage 31:993-1003.

Lintl P, Braak H (1983) Loss of intracortical myelinated fibers: a distinctive age-related alteration in the human striate area. Acta Neuropathol 61:178-182.

MacDonald SW, Li SC, Backman L (2009) Neural underpinnings of within-person variability in cognitive functioning. Psychol Aging 24:792-808.

Marcus DS, Fotenos AF, Csernansky JG, Morris JC, Buckner RL (2010) Open access series of imaging studies: longitudinal MRI data in nondemented and demented older adults. J Cogn Neurosci 22:2677-2684.

Mather M, Cacioppo JT, Kanwisher N (2013) How fMRI can inform cognitive theories. Perspect Psychol Sci 8:108-113.

Mesulam MM (1981) A cortical network for directed attention and unilateral neglect. Ann Neurol 10:309-325.

Montembeault M, Joubert S, Doyon J, Carrier J, Gagnon JF, Monchi O, Lungu O, Belleville S, Brambati SM (2012) The impact of aging on gray matter structural covariance networks. Neuroimage 63:754-759.

Pakkenberg B, Gundersen HJ (1997) Neocortical neuron number in humans: effect of sex and age. J Comp Neurol 384:312-320.

Panizzon MS, Fennema-Notestine C, Kubarych TS, Chen CH, Eyler LT, Fischl B, Franz CE, Grant MD, Hamza S, Jak A, Jernigan TL, Lyons MJ, Neale MC, Prom-Wormley EC, Seidman L, Tsuang MT, Wu H, Xian H, Dale AM, Kremen WS (2012) Genetic and environmental influences of white and gray matter signal contrast: a new phenotype for imaging genetics? Neuroimage 60:1686-1695.

Paus T (2005) Mapping brain maturation and cognitive development during adolescence. Trends Cogn Sci 9:60-68.

Paus T, Keshavan M, Giedd JN (2008) Why do many psychiatric disorders emerge during adolescence? Nat Rev Neurosci 9:947-957.

Peters A, Sethares C (2002) Aging and the myelinated fibers in prefrontal cortex and corpus callosum of the monkey. J Comp Neurol 442:277-291.

Peters A, Sethares C, Killiany RJ (2001) Effects of age on the thickness of myelin sheaths in monkey primary visual cortex. J Comp Neurol 435:241-248.

Raz N, Lindenberger U, Rodrigue KM, Kennedy KM, Head D, Williamson A, Dahle C, Gerstorf D, Acker JD (2005) Regional Brain Changes in Aging Healthy Adults: General Trends, Individual Differences and Modifiers. Cereb Cortex %R 101093/cercor/bhi044 15:1676-1689.

Sacerdot.Ed (1974) Planning in a Hierarchy of Abstraction Spaces. Artif Intell 5:115-135.

Salat DH, Lee SY, van der Kouwe AJ, Greve DN, Fischl B, Rosas HD (2009) Age-associated alterations in cortical gray and white matter signal intensity and gray to white matter contrast. Neuroimage 48:21-28.

Salat DH, Chen JJ, van der Kouwe AJ, Greve DN, Fischl B, Rosas HD (2011) Hippocampal degeneration is associated with temporal and limbic gray matter/white matter tissue contrast in Alzheimer's disease. Neuroimage 54:1795-1802.

Salthouse TA (1996) The processing-speed theory of adult age differences in cognition. Psychol Rev 103:403-428.

Schlaug G (2001) The brain of musicians. A model for functional and structural adaptation. Ann N Y Acad Sci 930:281-299.

Segonne F, Dale AM, Busa E, Glessner M, Salat D, Hahn HK, Fischl B (2004) A hybrid approach to the skull stripping problem in MRI. Neuroimage 22:1060-1075.

Shaw P, Greenstein D, Lerch J, Clasen L, Lenroot R, Gogtay N, Evans A, Rapoport J, Giedd J (2006) Intellectual ability and cortical development in children and adolescents. Nature 440:676-679.

Shimamura AP (2010) Bridging Psychological and Biological Science: The Good, Bad, and Ugly. Perspectives on Psychological Science 5:772-775.

Shing YL, Werkle-Bergner M, Brehmer Y, Muller V, Li SC, Lindenberger U (2010) Episodic memory across the lifespan: the contributions of associative and strategic components. Neurosci Biobehav Rev 34:1080-1091.

Sled JG, Zijdenbos AP, Evans AC (1998) A nonparametric method for automatic correction of intensity nonuniformity in MRI data. IEEE Trans Med Imaging 17:87-97.

Song SK, Yoshino J, Le TQ, Lin SJ, Sun SW, Cross AH, Armstrong RC (2005) Demyelination increases radial diffusivity in corpus callosum of mouse brain. Neuroimage 26:132-140.

Sowell ER, Peterson BS, Thompson PM, Welcome SE, Henkenius AL, Toga AW (2003) Mapping cortical change across the human life span. Nat Neurosci 6:309-315.

Sporns O (2012) Discovering the Human Connectome. Cambridge, MA: MIT Press.

Sporns O, Honey CJ, Kotter R (2007) Identification and classification of hubs in brain networks. PLoS One 2:e1049.

Stuss DT, Murphy KJ, Binns MA, Alexander MP (2003) Staying on the job: the frontal lobes control individual performance variability. Brain 126:2363-2380.

Tamnes CK, Fjell AM, Westlye LT, Ostby Y, Walhovd KB (2012) Becoming consistent: developmental reductions in intraindividual variability in reaction time are related to white matter integrity. The Journal of neuroscience : the official journal of the Society for Neuroscience 32:972-982.

Tamnes CK, Ostby Y, Fjell AM, Westlye LT, Due-Tonnessen P, Walhovd KB (2010) Brain maturation in adolescence and young adulthood: regional age-related changes in cortical thickness and white matter volume and microstructure. Cereb Cortex 20:534-548.

Treves A (2005) Frontal latching networks: a possible neural basis for infinite recursion. Cogn Neuropsychol 22:276-291.

van den Heuvel MP, Sporns O (2011) Rich-club organization of the human connectome. The Journal of neuroscience : the official journal of the Society for Neuroscience 31:15775-15786.

van den Heuvel MP, Kahn RS, Goni J, Sporns O (2012) High-cost, high-capacity backbone for global brain communication. Proc Natl Acad Sci U S A 109:11372-11377.

Van Petten C (2004) Relationship between hippocampal volume and memory ability in healthy individuals across the lifespan: review and meta-analysis. Neuropsychologia 42:1394-1413.

Walhovd KB, Fjell AM, Reinvang I, Lundervold A, Fischl B, Quinn BT, Dale AM (2004) Size does matter in the long run: hippocampal and cortical volume predict recall across weeks. Neurology 63:1193-1197.

Walhovd KB, Fjell AM, Dale AM, McEvoy LK, Brewer J, Karow DS, Salmon DP, Fennema-Notestine C (2008) Multi-modal imaging predicts memory performance in normal aging and cognitive decline. Neurobiol Aging.

Walters NB, Egan GF, Kril JJ, Kean M, Waley P, Jenkinson M, Watson JD (2003) In vivo identification of human cortical areas using high-resolution MRI: an approach to cerebral structure-function correlation. Proc Natl Acad Sci U S A 100:2981-2986.

Wechsler D (1999) Wechsler Abbreviated Scale of Intelligence. San Antonio, TX: The Psychological Corporation.

Westlye LT, Grydeland H, Walhovd KB, Fjell AM (2011) Associations between regional cortical thickness and attentional networks as measured by the attention network test. Cereb Cortex 21:345-356.

Westlye LT, Walhovd KB, Dale AM, Espeseth T, Reinvang I, Raz N, Agartz I, Greve DN, Fischl B, Fjell AM (2009) Increased sensitivity to effects of normal aging and Alzheimer's disease on cortical thickness by adjustment for local variability in gray/white contrast: a multi-sample MRI study. Neuroimage 47:1545-1557.

Westlye LT, Walhovd KB, Dale AM, Bjornerud A, Due-Tonnessen P, Engvig A, Grydeland H, Tamnes CK, Ostby Y, Fjell AM (2010a) Life-span changes of the human brain white matter: diffusion tensor imaging (DTI) and volumetry. Cereb Cortex 20:2055-2068.

Westlye LT, Walhovd KB, Dale AM, Bjornerud A, Due-Tonnessen P, Engvig A, Grydeland H, Tamnes CK, Ostby Y, Fjell AM (2010b) Differentiating maturational and aging-related changes of the cerebral cortex by use of thickness and signal intensity. Neuroimage 52:172-185.

Yakovlev PI, Lecours A-R (1967) The myelogenic cycles of regional maturation of the brain. In: Regional Development of the Brain in Early Life (Minkowski A, ed), pp 3-70. Oxford and Edinburg: Blackwell Scientific Publications.

Zalc B, Colman DR (2000) Origins of vertebrate success. Science 288:271-272.

Zalesky A, Fornito A, Harding IH, Cocchi L, Yucel M, Pantelis C, Bullmore ET (2010) Whole-brain anatomical networks: does the choice of nodes matter? Neuroimage 50:970-983.

Zielinski BA, Gennatas ED, Zhou J, Seeley WW (2010) Network-level structural covariance in the developing brain. Proc Natl Acad Sci U S A 107:18191-18196.

10. Papers I-III

II

Behavioral/Cognitive

Intracortical Myelin Links with Performance Variability across the Human Lifespan: Results from T1- and T2-Weighted MRI Myelin Mapping and Diffusion Tensor Imaging

Håkon Grydeland, Kristine B. Walhovd, Christian K. Tamnes, Lars T. Westlye, and Anders M. Fjell
Research Group for Lifespan Changes in Brain and Cognition, Department of Psychology, University of Oslo, 0317 Oslo, Norway

Cerebral myelin maturation and aging-related degradation constitute fundamental features of human brain integrity and functioning. Although mostly studied in the white matter, the cerebral cortex contains significant amounts of myelinated axons. However, how intracortical myelin content evolves during development, decays in aging, and links with cognition remain poorly understood. Several studies have shown the potential of mapping myelin in the cortex by use of T1-weighted (T1w) and T2-weighted (T2w) magnetic resonance imaging signal intensity, which show inverse sensitivity to myelin. Here, we characterized cortical myelin in 339 participants 8–83 years of age using a recently introduced T1w/T2w ratio myelin mapping technique and mean diffusivity (MD) from diffusion tensor imaging. To test for cognitive correlates, we used intraindividual variability (IIV) in performance during a speeded task, a measure recently associated with white matter integrity. The results showed that intracortical myelin maturation was ongoing until the late 30s, followed by 20 relative stable years before declining from the late 50s. For MD, U-shaped paths showing similar patterns were observed, but with fewer maturational effects in some regions. IIV was correlated with both T1w/T2w ratio and MD, mainly indicating that the higher degree of intracortical myelin is associated with greater performance stability. The relations were more prominent with advancing age, suggesting that aging-related cortical demyelination contributes to increased IIV. The T1w/T2w ratio myelin-mapping technique thus seems sensitive to intracortical myelin content in normal development and aging, relates to cognitive functioning, and might constitute an important future tool in mapping normal and clinical brain changes.

Introduction

Although most prominent in the white matter (WM) of the brain, myelinated axons abound within the cerebral cortex (Vogt, 1910; Nieuwenhuys, 2013). Cortical myelin maturation and aging-related degradation thus likely constitute fundamental features of how the brain evolves and devolves ontogenetically. Histology studies have shown protracted development of intracortical myelination in humans (Yakovlev and Lecours, 1967) and aging-related cortical myelin alterations in primates (Feldman and Peters, 1998). The observation of prolonged myelination makes intracortical axons particularly interesting to investigate in a lifespan perspective (Bartzokis, 2004). However, attempts to map intracortical lifespan trajectories of myelin *in vivo* are lacking and a link with cognitive functioning has not been established.

Magnetic resonance imaging (MRI) facilitates *in vivo* noninvasive whole-brain characterization of large samples. How cortical integrity changes with age and relates to cognitive abilities have in MRI studies usually been investigated using cortical thickness or volume (Bartzokis et al., 2001; Sowell et al., 2003; Gogtay et al., 2004; Carreiras et al., 2009; Fjell et al., 2009; Tamnes et al., 2010; Kochunov et al., 2011; Westlye et al., 2011). Although putatively also partly reflecting myelin (Paus, 2005), these measures have limited neurobiological specificity. Indices derived from diffusion tensor imaging (DTI) have been associated more directly, although far from exclusively (Beaulieu, 2002), with myelin (Song et al., 2002), but have primarily been used to map WM or subcortical gray matter (GM) structures (Westlye et al., 2010a; Kochunov et al., 2011; Lebel and Beaulieu, 2011).

Interestingly, cortical regions can be delineated based on myelin content by use of intrinsic signal intensity properties of T1-weighted (T1w) or T2-weighted (T2w) MRI (Yoshiura et al., 2000; Sigalovsky et al., 2006). A recent study created detailed surface-based cortical myelin maps by taking a ratio of T1w and T2w image intensities to correct for the MRI-related image intensity bias field and to increase the contrast to noise ratio for myelin (Glasser and Van Essen, 2011).

Received July 2, 2013; revised Sept. 30, 2013; accepted Oct. 23, 2013.

Author contributions: H.G., K.W., and A.M.F. designed research; H.G., C.K.T., and L.T.W. performed research; H.G., C.K.T., L.T.W., and A.M.F. analyzed data; H.G., K.W., C.K.T., L.T.W., and A.M.F. wrote the paper.

This work was supported by The Norwegian Research Council (to K.B.W., L.T.W., and A.M.F.) and the European Research Council Starting Grant Scheme (to K.B.W. and A.M.F.).

The authors declare no competing financial interests.

Correspondence should be addressed to Håkon Grydeland, Department of Psychology, University of Oslo, PO Box 1094, Blindern, 0317 Oslo, Norway. E-mail: hakon.grydeland@psykologi.uio.no.

L.T. Westlye's present address: Norwegian Centre for Mental Disorders Research (NORMENT), K.G. Jebsen Centre for Psychosis Research, Division of Mental Health and Addiction, Oslo University Hospital, and Department of Psychology, University of Oslo, 0317 Oslo, Norway.

DOI:10.1523/JNEUROSCI.2811-13.2013

 0270-6474/13/3318618-13$15.00/0

Table 1. Sample characteristics

	N (% female)	Age, y	Education, y[a]	MMSE[b]	Full-scale IQ
Young	85 (50.6)	14.7 (3.3; 8.4–19.7)	NA	NA	108.9 (9.9; 91–132)
Adults	254 (57.3)	48.8 (17.0; 19.7–83.1)	15.7 (2.8; 4–26)	29.2 (0.8; 26–30)	114.2 (8.6; 92–141)
Total	339 (55.5)	40.3 (20.9; 8.4–83.1)	15.7 (2.8; 4–26)	29.2 (0.8; 26–30)	112.8 (9.2; 91–141)

Data are shown as mean (SD; min-max) if not otherwise indicated. NA, not applicable.

[a]Missing from two adult subjects.

[b]Available for subjects >40 years of age.

Therefore, the cortex was parcellated based on local differences in myelin content derived from MRI alone. This myelin-mapping approach allows for addressing tantalizing questions of how intracortical myelin influences cognitive functioning and how this relation unfolds across the lifespan. Recently, we demonstrated an association between WM integrity and intraindividual variability (IIV) in performance during a speeded performance task (Fjell et al., 2011; Tamnes et al., 2012). However, whether these effects relate specifically to the WM fiber pathways connecting distributed brain regions remain unknown; that degree of cortical myelin contributes to the individual differences in performance stability constitutes an intriguing but untested hypothesis.

The present study aimed to: (1) delineate intracortical myelination through the lifespan using the T1w/T2w ratio launched by Glasser and Van Essen (2011) and (2) assess the association between cognitive performance variability and intracortical myelin grade. In addition, all analyses were also performed with DTI-derived mean diffusivity (MD) values from the same cortical areas. We hypothesize an inverted U-shaped trajectory of cortical myelin across the lifespan and that higher myelin grade yields less performance variability, particularly with advancing age (Fjell et al., 2011).

Materials and Methods

Subjects. The Regional Committee for Medical and Health Research Ethics approved the study. We drew the sample from the first wave of two ongoing longitudinal projects by the Research Group for Lifespan Changes in Brain and Cognition at the University of Oslo, namely "Neurocognitive Development" and "Cognition and Plasticity through the Lifespan." Participants were recruited through newspaper ads, among students and employees at the University of Oslo, and from local schools. Further details regarding recruitment and enrollment were described previously (Westlye et al., 2009a; Tamnes et al., 2010). Participants <12 years of age gave oral informed consent, whereas written informed consent was obtained from all participants >12 years of age and from a parent or guardian for participants <18 years of age. Participants <16 years of age and their parents were screened with standardized health interviews to ascertain eligibility; we required participants to be right-handed, fluent Norwegian speakers, and have normal or corrected to normal vision and hearing. Self-reported (screening interview at enrollment) neurological or psychiatric conditions known to affect normal cerebral functioning, including clinically significant stroke, traumatic brain injury, untreated hypertension, diabetes, use of psychoactive drugs within the last 2 years, or worries concerning own cognitive status including memory function, were exclusion criteria. All participants >20 years of age scored <16 on the Beck Depression Inventory (Beck and Steer, 1987) and participants >40 years of age scored ≥ 26 on the Mini Mental State Examination (Folstein et al., 1975). A neuroradiologist evaluated and deemed all scans free of significant injuries or conditions in all but three cases, which were excluded. Of the remaining 400 participants satisfying these criteria, 61 subjects were excluded due to incomplete records (missing behavioral assessment or T1w, T2w, or DTI scans), motion-compromised MRI data (determined by visual inspection), age (one participant exceeded 90 years, creating a gap of missing data points on the otherwise continuous age scale), or suboptimal task focus or performance (in the young subsample) defined as <80% accuracy in the congruent trials or a nonsignificant congruency effect on reaction time (RT) in correct trials (i.e., faster responses for congruent compared with incongruent trials; see description of task below). The suboptimal task performance criteria resulted in the exclusion of 9 participants (mean age = 11.1 years, SD = 2.3 years, min-max 8.8–14.5 years) and were applied in the young subsample to ensure that participants having difficulties in performing the task adequately did not unduly influence the brain–behavior associations. In total, we included 339 participants (188 females, 55.5%; Table 1), mean age = 40.3, SD = 20.9, min-max age = 8.4–83.1. A two-sample *t* test revealed no significant differences in age between females (mean age = 41, SD = 20.3) and males (mean age = 39.6, SD = 21.8; $t_{(337)} = 0.624$, $p = 0.53$). To facilitate comparisons with our previous studies using overlapping samples (Fjell et al., 2011; Tamnes et al., 2012), we created similar age range subsamples: young ($n = 85$, 43 females [50.6%], mean age = 14.7, SD = 3.3, min-max age = 8.4–19.7) and adults ($n = 254$, 146 females [57.3%], mean age = 48.8, SD = 17.0, min-max age = 19.7–83.1).

General cognitive abilities were assessed by Wechsler Abbreviated Scale of Intelligence (Wechsler, 1999). Estimated mean full-scale intelligence quotient (FIQ) for the entire sample was 112.8 (range = 91–141, SD = 9.2).

Image acquisition. MRI was performed using a 12-channel head coil on a 1.5 T Siemens Avanto scanner at Oslo University Hospital Rikshospitalet. The T1w volumes were acquired using a 3D T1w magnetization-prepared rapid gradient echo (MPRAGE; TR = 2400 ms, TE = 3.61 ms, TI = 1000 ms, 8° flip angle, bandwidth = 180 Hz/pixel, FOV = 240 mm, matrix = 192 × 192 × 160, 1.25 × 1.25 × 1.2 mm voxels). For the T2w volumes, a 3D T2w sampling perfection with application-optimized contrasts using different flip angle evolutions (SPACE, TR = 3390 ms, TE = 388 ms, variable flip angle, bandwidth = 650 Hz/pixel, FOV = 256 mm, 1 mm isotropic voxels) was used; 155 participants (46.6%) were scanned with a 204 × 256 × 176 matrix (mean age = 37.5, SD = 19.0, min-max = 8.4–60.6), and 151 participants (53.4%) were scanned with a 256 × 256 × 176 matrix (mean age = 42.8, SD = 22.3, min-max = 8.5–83.1). All other T2w parameters were equal. Both T1w and T2w scans were acquired sagittally.

The DTI was performed with a single-shot twice-refocused spin-echo echo planar imaging pulse sequence with 30 diffusion-sensitized gradient directions (TR = 8200 ms, TE = 82 ms, b-value = 700 s/mm^2, 2 mm isotropic voxels, and 64 axial slices). The sequence, optimized to minimize eddy current-induced distortions (Reese et al., 2003), was repeated in 2 successive runs with 10 b = 0 and 30 diffusion weighted images collected per run.

Preprocessing. All datasets were processed and analyzed at the Neuroimaging Analysis Laboratory, Research Group for Lifespan Changes in Brain and Cognition, University of Oslo. The original unresampled T1w volumes were processed using the Freesurfer 5.1 suite (http://surfer.nmr.mgh.harvard.edu), performing brain extraction, intensity normalization, automated tissue segmentation, surface-based cortical thickness estimations, generation of white and pial surfaces, surface topology correction, automated whole-brain segmentation, and spherical interindividual surface alignment (Sled et al., 1998; Dale et al., 1999; Fischl et al., 1999a; Fischl and Dale, 2000; Fischl et al., 2002; Fischl et al., 2004a; Fischl et al., 2004b; Ségonne et al., 2004).

The T2w image was registered to the unresampled T1w image by using Freesurfer's *bbregister*, a within-subject, cross-modal registration using a boundary-based cost function constrained to be six degrees of freedom (rigid body; Greve and Fischl, 2009). The resulting linear transform was applied by use of FSL's *applywarp* tool using spline interpolation which minimize the white matter and CSF contamination of GM voxels that would result from the volumetric blurring inherent in trilinear interpolation (Glasser and Van Essen, 2011).

The T1w volume was then divided on the aligned preprocessed T2w volume, creating a T1w/T2w ratio volume. Based on recent work on T1w signal

intensity by us (Westlye et al., 2009b) and others (Panizzon et al., 2012), we sampled T1w/T2w values vertex-wise at a distance of 0.2 mm into the GM from the WM/GM boundary using Freesurfer's *mri_vol2surf* tool, yielding T1w/T2w ratio surfaces. This fixed distance procedure diverge from the mid-thickness-based average approach taken by Glasser and Van Essen (2011). However, in the present data, after inspecting age-trajectory curves based on average values (sampled at 20 steps along the normal spaced at 0.05 fraction intervals), we found that a fixed distance approach was less prone to interactions of age, thickness, and intensity; such interaction effects would be expected to be more readily present when studying lifespan trajectories compared with the more narrow age span in the samples used by Glasser and Van Essen of mean age 22 ± 6 years and 42 ± 11 years. Further, as we previously have found effects of WM microstructure on IIV, we included measurements of WM T1w/T2w as a per-vertex regressor in our model to assess for potential cortical-specific effects (see below). Therefore, we sampled WM T1w/T2w values at a 1.0 mm distance from the WM/GM boundary into the WM, creating WM T1w/T2w surfaces.

DTI has emerged as a widely applied and validated method of assessing brain microstructure (Concha et al., 2006). DTI-derived indices have been linked to myelin (Song et al., 2005), but likely primarily reflect other microstructural properties such as axon fiber diameter and density (Beaulieu, 2002). Therefore, even if not being predominantly a measure of myelin, DTI is a viable way of measuring microstructural changes over the lifespan (Lebel et al., 2012). Although challenges exist in estimating diffusivity in the cortex due to partial-volume effects (Koo et al., 2009), it has been successfully applied to detect GM alterations in, for example, aging (Abe et al., 2008). Therefore, we included DTI measurements to allow for comparisons of the new T1w/T2w ratio method with a previously established method of microstructure assessment.

DTI image analyses and tensor calculations were done using FSL (Smith et al., 2004; Woolrich et al., 2009). Each volume was affine registered to the T2-weighted b = 0 volume using FLIRT (Jenkinson and Smith, 2001) correcting for motion between scans and residual eddy-current distortions. After removal of nonbrain tissue (Smith, 2002) eigenvector and eigenvalue maps were computed. We chose MD, the mean of the eigenvalues $[(\lambda1 + \lambda2 + k\lambda)/3]$, as the measure of interest because GM has been shown have low values of anisotropy (Pierpaoli et al., 1996), thus potentially making other sensitive and commonly used indices such as fractional anisotropy and radial diffusivity (Grydeland et al., 2010) less informative. The first T2-weighted b = 0 volume was registered to the unresampled T1w volume in the same way as the T2w image, and the resulting transform was then used to register the MD volume to the T1w volume. The MD values were subsequently sampled in an identical manner to the T1w/T2w values.

All individual surfaces (cortical T1w/T2w, WM T1w/T2w, MD, and thickness maps) were mapped to a common surface using a nonrigid, high-dimensional spherical averaging method to align cortical folding patterns (Fischl et al., 1999a; Fischl et al., 1999b), smoothed with a circularly symmetric Gaussian kernel across the surface using a full width at half maximum of 12 mm, and fed to statistical analyses. To perform curve-fitting analyses for visualization of the estimated lifespan trajectories, we divided the surface into 33 gyral-based areas in each hemisphere (Fischl et al., 2004b; Desikan et al., 2006) and averaged the measures of interest within selected cortical parcellations.

Experimental task. We administered a modified version of the Eriksen flanker task (Eriksen and Eriksen, 1974), similar to the task used by Debener et al. (2005), described in detail previously (Westlye et al., 2009a). The procedure and preprocessing steps are identical to, and previously described in, Fjell et al. (2011) and Tamnes et al. (2012) for the adult and young subsample, respectively. Briefly, horizontal arrows (length = 1°) pointing either to the left or the right were displayed centrally on a computer screen in a vertical stack 2.5° high. Subjects were instructed to respond as accurately and quickly as possible by pressing one button if the target was pointing to the left and another button if the target was pointing to the right. Each trial consisted of a central fixation cross presented for a random interval ranging between 1200 and 1800 ms, followed by the presentation of four "flanker" arrows for 80 ms before the target arrow appeared in the middle of the stack of flanker arrows for 30 and 60 ms for the adult and young subsample, respectively. The flanker arrows were presented before the target to increase prepotent responding and to make the task more difficult. A training session of 20 and 24 trials for the adult and young subsample, respectively, was administered to familiarize the participant with the task.

Responses were obtained on a PST Serial Response Box and the experimental procedures and responses were collected using E-prime software (Psychological Software Tools). The task included 416 trials with a short break halfway and there were two experimental task conditions, congruent and incongruent, with 208 trials each. In the congruent condition, all arrows pointed in the same direction. In the incongruent condition, the middle arrow pointed in the direction opposite of that of the flanker arrows. The probability of an incongruent trial was 50% in a randomized fashion. Because both Fjell et al. (2011) and Tamnes et al. (2012) found robust effects in both conditions, we here limited our analyses to values based on the congruent trials.

Based on the mean RT for the first 20 consecutive trials, an individually adjusted RT criterion was set (10% and 15% above mean RT of the 20 initial trials for the adult and the young subsample, respectively). After every subsequent third trial with either RT exceeding this criterion or with response omission, a message occurred on screen for 1 s instructing the participant to respond faster. The rational for using this procedure was to increase the participants' motivation for rapid responses and to enhance their attentional investments in the task. We expected that this would lead to reduced variability due to random attentional drifts and leave us with a measure of variability more closely related to task-focused CNS function. Therefore, IIV in this task may be more related to the ability to respond in a constant and speedy manner rather than naturally occurring trial-to-trial variability.

For the statistical analyses, we excluded the first 10 trials and the 10 trials with the fastest and slowest RTs for each subject because it is difficult to decide whether extreme responses represent variations of the real cognitive processes under study or if they result from random noise due to factors such as the participant missing the button, having a single lapse of attention during the course of a long speeded task, etc. Although such instances of attention lapses likely reflect a phenomenon of interest, the difficulty in discerning it from missed button press and other random noise constitutes a challenge. Therefore, a simple way of reducing the possibility that noise contaminate the data without biasing the results in either direction (although at a cost of leaving out potentially interesting data) is to exclude the extreme ends of the RT distribution for all participants. The approach does not, however, completely preclude the presence of extreme values beyond the 10 fastest and 10 slowest RTs, although if present, these are likely of a limited number with negligible impact on the data. As in our previous studies (Fjell et al., 2011; Tamnes et al., 2012), for the resulting trials, we operationalized IIV by calculating the SD of the RT (sdRT) as the measure of interest; median RT (mRT) was included as a covariate in all analyses to control for effects of reaction time because a relationship between sdRT and mRT is expected (for a discussion related to the quantification of IIV, see MacDonald et al., 2009). Median RT was preferred to mean RT because RT generally does not follow strict normal distribution but has a thicker tail of slow compared with fast values. In the present dataset, the correlation between the median and the mean RT was 0.995 and 0.960 in the adult and the young subsample, respectively.

Statistics. For the entire sample, we applied general linear models (GLMs) to test for expected (Westlye et al., 2010b) quadratic effects of age (age^2) on the cortical T1w/T2w ratio and MD maps at each vertex with terms for the linear effects of age and sex as global covariates. For the T1w/T2w ratio analyses, we first estimated the effect of difference in T2w matrix across the whole sample to minimize potential confounds with age and the subsample analyses were performed on the resulting residuals. Cortical thickness was included as a per-vertex regressor in all GLMs. To estimate age trajectories without any assumption about the form of the curve, we fitted a nonparametric local smoothing model, the smoothing spline, implemented in MATLAB (MathWorks), to the mean values of representative regions of interest (ROI) across the mantle. We calculated *z*-scores from the residuals after modeling the effect of T2w matrix type and plotted the mean values across hemispheres per ROI. We have shown previously that the smoothing spline approach yields less biased solutions than the more commonly used higher order polynomial functions (Fjell et al., 2010). We used

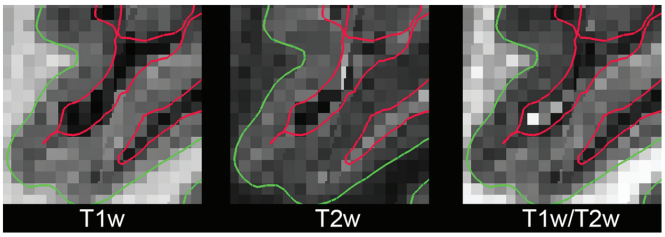

Figure 1. T1w, T2w, and T1w/T2w volumes. Shown is a section of a T1w, T2w, and T1w/T2w volume, respectively, illustrating the highly myelinated transverse temporal part of the superior temporal lobe (the middle gyrus, denoted with an asterisk in the T1w) evidencing lighter, darker, and lighter intensity, respectively, than the surrounding cortical tissue. The green surface denotes the sampling distance of 0.2 and the red line represents the GM/CSF boundary.

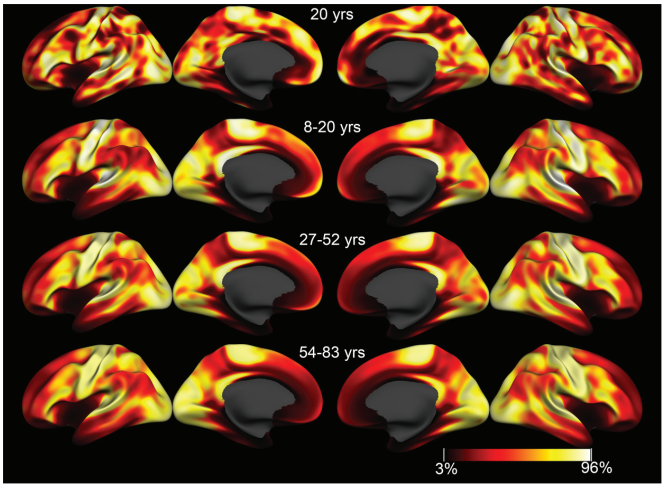

Figure 2. T1w/T2w ratio surface maps. Shown are T1w/T2w ratio surface maps from a female 20 years of age overlaid on a semi-inflated surface. Average T1w/T2w ratio surface of maps of the young subsample ($n = 85$, age 8.3–19.7 years), middle-aged participants ($n = 85$, age 27.4–51.7 years), and the oldest participants ($n = 85$, age 58.4–83.1 years). T1w/T2w ratio values below the third percentile and above the 96th percentile, calculated across participants, are sat to saturation (dark and light, respectively).

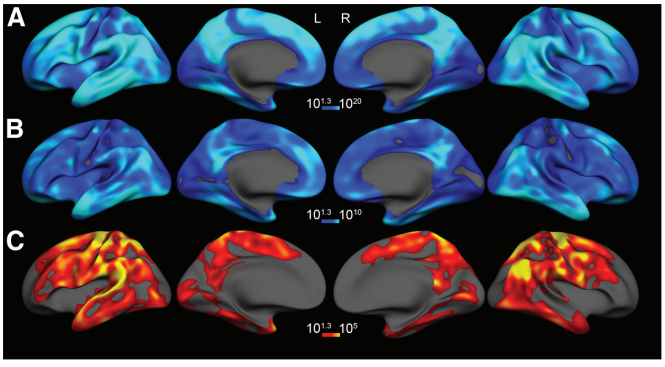

Figure 3. T1w/T2w myelin ratio and age. *p*-value maps are overlaid on semi-inflated brains showing the relationship between T1w/T2w myelin ratio and the quadratic effects of age in all subjects (age 8–83 years; ***A***), the quadratic effects of age in the adult subsample (age 20–83 years; ***B***), and the linear effects of age in the young subsample (age 8–19 years; ***C***), respectively. The effects are corrected for multiple comparisons, but actual *p*-values are shown. See Table 2 for cluster-wise *p*-values.

an algorithm that optimizes smoothing level based on a version of Bayesian Information Criterion, which provides a way of obviating the need for arbitrarily chosen smoothing levels. The following distributed ROIs were chosen to cover distributed parts of the cortical mantle and to allow comparison with Westlye et al. (2010b): superior frontal, rostral middle frontal, paracentral, superior parietal, inferior temporal, isthmus cingulate, parahippocampal, pericalcarine, and insula. Similarly, we also performed the smoothing spline fitting at each vertex, saved age at the peak (highest T1w/T2w ratio value) on the resulting curve, and displayed the results as surface maps to give an even more detailed picture of the transition between development and aging. To probe the relationship between intracortical myelin and IIV, we tested linear effects of sdRT on T1w/T2w ratio and MD values with GLMs while regressing out mRT, sex, and age, and thickness per-vertex. We ran GLMs to explicitly test whether the relationship between sdRT and T1w/T2w ratio and MD, respectively, changed with age. The age × sdRT interaction term was included in the analyses, using sex, age, mRT, sdRT, and thickness per-vertex as covariates. We repeated the IIV analyses including WM T1w/T2w as per-vertex regressor to assess for potential cortical-specific effects. For all surface analyses, the data were tested against an empirical null distribution of maximum cluster size across 10,000 iterations using Z Monte Carlo simulations as implemented in FreeSurfer (Hagler et al., 2006) synthesized with a cluster-forming threshold of $p < 0.05$ (two-sided), yielding clusters corrected for multiple comparisons across the surfaces with corresponding cluster-wise *p*-values. To illustrate the individual data points and to provide a general measure of effect size, we extracted values from significant cluster vertices and plotted against sdRT. These correlation analyses were restricted to vertices for which the values were already to be significantly related to IIV and thus must not be regarded as part of the hypothesis testing, but rather as a suitable way of estimating effect sizes. Finally, we tested the robustness of the behavioral associations and the potential effects of general intellectual functioning by entering the mean values in a regression, calculating studentized deleted residuals, excluding cases exceeding ± 2.5 (which was considered more stringent than a Bonferroni-corrected cutoff value) and rerunning the regression including FIQ as a covariate (together with age, sex, and cortical thickness). Specifically, we tested whether removing potential outliers and including FIQ would remove the statistical relationship between microstructure and IIV.

Results

Intracortical T1w/T2w ratio myelin and age

Figure 1 shows excerpt from T1w, T2w, and T1w/T2w volumes from a female 20 years of age; Figure 2 shows T1w/T2w ratio surface maps for the same female and 3-group average maps of 85 subjects each, 8–20, 27–52, and 58–83 years of age, respectively.

Figure 3*A* displays *p*-value maps of intracortical T1w/T2w as a function of age^2 in each vertex across all subjects, with age and sex as global covariates and cortical thickness as a per-vertex regressor. Widespread negative quadratic effects, indicating an inverted U-shaped relationship between T1w/T2w ratio and age, were found, covering ~91% the vertices in each hemisphere (for details, see Table 2). Specifically, the strongest effects were observed in frontal, parietal, and temporal association areas, whereas primary sensory areas showed weaker effects. We repeated the quadratic analysis of age in only the adult subsample and tested for the linear effects of age in the young subsample. In the adults (Fig. 3*B*), the quadratic effects were similar, but naturally statistically weaker, compared with the whole sample. In the youngest subsample (Fig. 3*C*), widespread linear effects comprising 81% and 74% of the vertices in the left and right hemisphere, respectively, were found, indicating increasing T1w/T2w ratio with age. Effects were prominent particularly in posterior frontal, parietal, and temporal cortices; weaker or no effects were found in parts of anterior frontal, insular, and lateral occipital cortices.

Figure 4 illustrates the lifespan T1w/T2w ratio trajectories in the selected ROIs showing the fitted smoothing spline curve. The majority of regions showed an inverted U-shaped T1w/T2w ratio trajectory across life: a steep increase until the end of the 30s, followed by a relatively stable period, before a decrease from the end of the 50s. Deviating somewhat from this pattern, the parahippocampal and paracentral cortex showed a more protracted increase and a less steep decline around the sixth decade, whereas the pericalcarine cortex trajectory did not evidence any decrease, instead increasing quite linearly through the whole age range. Figure 5 depicts surface maps showing the age of the transition between development and aging-related decline in T1w/T2w ratio after fitting the same smoothing spline at each vertex. Superior frontal, inferior parietal and temporal, and posterior cingulate cortices demonstrated the earliest signs of transition, whereas heavily myelinated primary sensory areas did not show decline.

Figure 6 shows WM T1w/T2w ratio age trajectories in the same selected ROIs as for GM T1w/T2w. In general, the curves show a less protracted development than the GM curves, but a similar though somewhat more pronounced decline from the late 50s. The mean correlation between WM and GM T1w/T2w across vertices was similar in the left and right hemisphere: 0.61 for adults and 0.67 for the young. In the adults, there was a trend for an increase in the correlations with age: 0.58 in adults below adult median age (52 years), and 0.70 above (p-value of difference between correlations = 0.06, one-tailed).

Intracortical MD and age

Figure 7*A* depicts *p*-value maps of intracortical DTI-derived MD as function of age^2 in each vertex across all subjects, with age and sex as global regressors and cortical thickness as a per-vertex regressor. Positive relationships indicating a U-shaped trajectory across age was found in 83% of the vertices in the left hemisphere and 86% in the right (for details, see Table 2). The strongest effects were seen in middle and superior frontal, cingulate, supramarginal, and inferior parietal cortices, generally bilateral but with slightly more pronounced right lateral prefrontal effects. Again, we repeated the analyses in the adult and young subsample separately: widespread quadratic effects (74% and 78% of the vertices in the left and right hemisphere, respectively) of age on MD were again found in the adults (Fig. 7*B*). The positive effects, reflecting a U-shaped relationship with age, were particularly strong in superior frontal, cingulate, precuneal, supramarginal, parietal, insular, and lateral occipital cortices. Weaker or no ef-

Table 2. Significant cluster details

Region Max Vtx (hemi)	% Vtx	Max *p*-value	CWP
T1w/T2w			
All − age^2			
Inferior parietal (lh)	90.7	−30.8	0.0001
Inferior parietal (rh)	90.6	−32.6	0.0001
Adults − age^2			
Superior frontal (lh)	89.1	−13.8	0.0001
Superior frontal (rh)	88.5	−12.8	0.0001
Young − age			
Postcentral (lh)	81.1	13.3	0.0001
Precentral (rh)	73.8	13.1	0.0001
Adults − IIV			
Lingual (lh)	2.5	−3.3	0.0028
Superior temporal (rh)	5.7	−4.5	0.0001
Insula	2.2	−3.9	0.0455
Supramarginal	4.2	−3.1	0.0003
Postentral	2.8	−3.0	0.0113
Young − IIV			
Lateral occipital (lh)	12.5	4.1	0.0001
Postcentral	4.9	2.9	0.0001
Superior parietal (rh)	11.2	4.2	0.0001
Postcentral	2.5	3.4	0.0368
Adults − IIV WM cov			
Superior temporal (rh)	1.8	−4.0	0.0081
Young − IIV WM cov			
Superior parietal (lh)	14.7	4.0	0.0001
Supramarginal	5.2	3.0	0.0001
Precentral	1.7	3.0	0.0327
Paracentral	2.0	3.0	0.0153
Superior parietal (rh)	12.0	3.8	0.0001
Postcentral	2.5	3.3	0.0025
Insula	1.7	3.2	0.0248
Adults − IIV × age			
Middle temporal (lh)	20.6	−4.5	0.0001
Supramarginal	4.1	−4.1	0.0004
Middle temporal (rh)	24.4	−5.4	0.0001
MD			
All − age^2			
Superior frontal (lh)	83.2	25.4	0.0001
Lateral orbitofrontal (rh)	85.8	33.4	0.0001
Adults − age^2			
Superior frontal (lh)	72.9	19.2	0.0001
Supramarginal (rh)	78.2	27.4	0.0001
Young − age			
Precentral (lh)	48.2	−10.7	0.0001
Lingual	0.9	6.2	0.0437
Precentral (rh)	41.7	−10.5	0.0001
Adults − IIV			
Pericalcarine (lh)	2.9	3.8	0.0001
Pars triangularis (rh)	3.6	4.6	0.0001
Lingual	1.3	3.1	0.0024
Young − IIV			
Pericalcarine (lh)	1.1	−5.4	0.0146
Precentral	4.8	4.4	0.0001
Superior frontal (rh)	1.7	3.6	0.0342
Precentral	2.3	3.1	0.0030
Pericalcarine	2.0	−2.9	0.0040
Adults − IIV × age			
Posterior cingulate (lh)	4.3	3.9	0.0001
Superior temporal	1.5	3.3	0.0341
Rostralmiddle frontal (rh)	4.3	4.9	0.0001
Entorhinal	1.5	4.9	0.0088
Precuneus	7.8	4.4	0.0001
Inferior parietal	12.5	4.1	0.0001
Precentral	1.4	3.1	0.0244
Lingual	1.8	2.4	0.0007

Region Max Vtx, region of maximum *p*-value vertex; hemi, hemisphere; % Vtx, percent of total vertices; Max *p*-value, maximum *p*-value (10^p) in cluster; CWP, clusterwise *p*-value (the *p*-value of the cluster); lh, left hemisphere; rh, right hemisphere. WM cov, WM T1w/T2w included as a covariate.

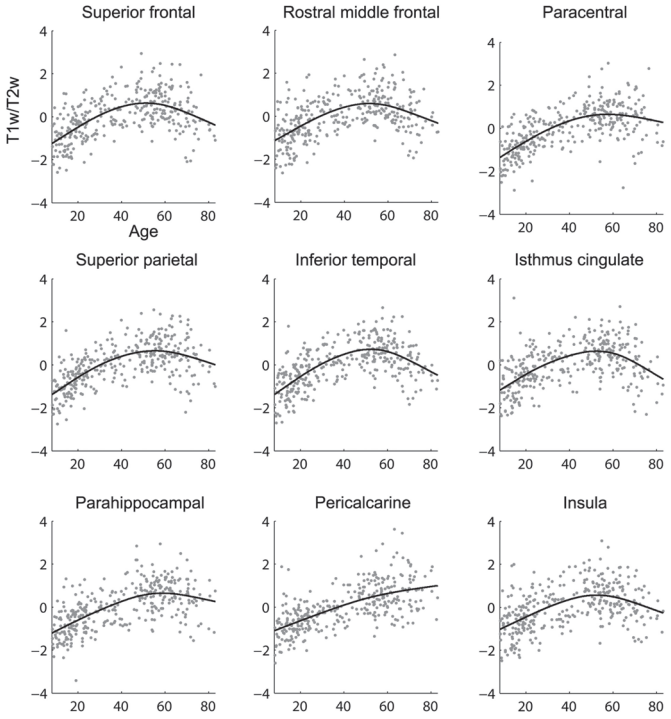

Figure 4. Lifespan T1w/T2w ratio trajectories in selected cortical ROIs. Values are standardized residual after regression of the T2w matrix; please see Materials and Methods for details. Age values are in years.

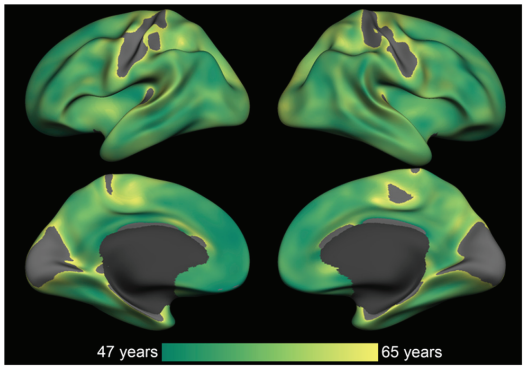

Figure 5. Development–aging transition. Surface maps show the age of the transition between development and aging. Vertexes not evidencing a peak before age 65 were set to a light gray color. The noncortical medial wall is set to a darker gray.

fects were apparent in temporal, around the central sulcus, and frontal pole cortices. In the young subsample (Fig. 7*C*), we observed negative linear effects in 48% and 42% of the vertices in the left and right hemisphere, respectively, particularly in precentral, superior temporal, superior frontal, and rostral middle frontal cortices, as well as medially in cingulate and precuneus cortices. A small cluster (1% of the vertices) showing marginally significant positive effects was also found peaking in the left lingual cortex, extending into pericalcarine cortex.

Figure 8 shows the lifespan mean MD trajectories in the same ROIs shown in Figures 4 and 6. The majority of regions show a U-shaped trajectory across life, the opposite of the T1w/T2w ratio pattern: a decrease in MD during the first decades of life, followed by a stable period, before an increase in MD with age starts around the sixth decade. Slight exceptions to this general pattern were seen in the paracentral, superior parietal, and pericalcarine cortices, none showing a decrease during the first two decades of life. The parahippocampal cortex, as for the T1w/T2w ratio, did not show any plateau, but an increase already from the early 20s.

Intracortical T1w/T2w ratio myelin and cognition

There were no differences across sex in sdRT (Mann–Whitney *U* test, adults: $z = -1.17$, $p = 0.200$; young, $z = 0.90$, $p = 0.367$) or mRT (adults: $z = -0.44$, $p = 0.662$); young: $z = 0.923$, $p = 0.356$). In the adults, age correlated positively with both sdRT ($r = 0.36$, $p < 10^{-8}$) and mRT ($r = 0.65$, $p < 10^{-31}$), but sdRT was not significantly related to age when controlling for mRT (estimate = 0.059, SE = 0.042, *t*-stat = 1.392, *p*-value = 0.165). In the young, age correlated negatively with sdRT ($r = -0.64$, $p < 10^{-10}$), even when controlling for mRT (estimate = −0.047, *p*-value = 0.008) and with mRT ($r = -0.62$, $p < 10^{-9}$).

To assess functional correlates of intracortical myelin, we performed similar analyses as in our previous studies, assessing the relationship between IIV and WM integrity separately for the adult and young subsample (Fjell et al., 2011; Tamnes et al., 2012). The results are presented in Figures 9 and 10 and in Table 2. In the adults, 1 cluster in the left hemisphere covering 2.5% of the vertices with peak in the lingual cortex extending medially into the temporal cortex showed a negative relationship between sdRT and T1w/T2w ratio (Fig. 9*A*). In the right hemisphere, four clusters covering 14.5% of the surface with peak values in superior temporal, insula, supramarginal, and postcentral cortices, respectively, showed a similar negative relationship. Therefore, higher variability in task performance was related to a lower T1w/T2w ratio, indicating reduced intracortical myelin, particularly in the right hemisphere. The relationships were of modest strength, with a mean Pearson product-moment correlation of −0.21 in both hemispheres. In the young subsample (Fig. 9*B*), two clusters covering 17.4% of the vertices peaking in the left lateral occipital and postcentral cortices and two right hemisphere clusters (13.1% of the vertices) with peaks in superior parietal and postcentral cortices showed a positive relationship between the T1w/T2w ratio and sdRT. Therefore, contrary to what was expected, increased variability in task performance was related to higher T1w/T2w ratio in these posterior regions. Correlations across clusters were 0.35 and 0.36 in the left and right hemispheres, respectively.

To investigate whether the relation between T1w/T2w and sdRT changed as a function of age, we added the interaction term age × sdRT to the previous linear model including age and sex as

global covariates and thickness as a per-vertex covariate. In the adults, two left hemisphere clusters comprising 25% of the vertices peaking in middle temporal and supramarginal cortices showed significant negative age interactions (Fig. 9*C*). This result indicates a stronger negative relationship between T1w/T2w and sdRT with increased age, as can be seen in the scatter plots in Figure 9*C*, in which the adult group has been divided based on the median age (52 years). One right hemisphere cluster spanning 24% of the vertices with maximum values in middle temporal cortex showed a similar age interaction. The mean correlations in the left and right hemisphere for the elderly were −0.09 and −0.12, respectively, and 0.06 and 0.04 in the young adults (<52 years), respectively. No interactions were found in the young subsample (<20 years).

All IIV-T1w/T2w ratio associations remained highly significant and correlations were generally unchanged when rerunning the regression after excluding studentized deleted residuals exceeding ±2.5. In the same model, FIQ did not yield a unique statistical contribution on T1w/T2w ratio (though showing a trend toward significance in one instance). Specifically, the IIV-T1w/T2w ratio correlations in the adults were similar in both the left (Pearson's *r* from −0.21 to −0.23; 6 cases exceeding the threshold of 2.5) and the right hemisphere (from −0.21 to −0.20, 7 cases exceeding the threshold). For the age-IIV interaction, the IIV-T1w/T2w ratio correlation in the young adults was slightly reduced in both the left (from 0.06 to 0.03, 8 cases exceeding the threshold) and the right hemisphere (0.04 to −0.02, 7 cases exceeding the threshold). For the oldest part of the adult subsample, there was a minor increase in the left hemisphere associations (from −0.09 to −0.11) and a large increase in right hemisphere associations (−0.12 to −0.21). For the youngest subsample, the left hemisphere IIV correlation was identical (0.35 in both instances), whereas the association in the right was clearly reduced (from 0.36 to 0.27).

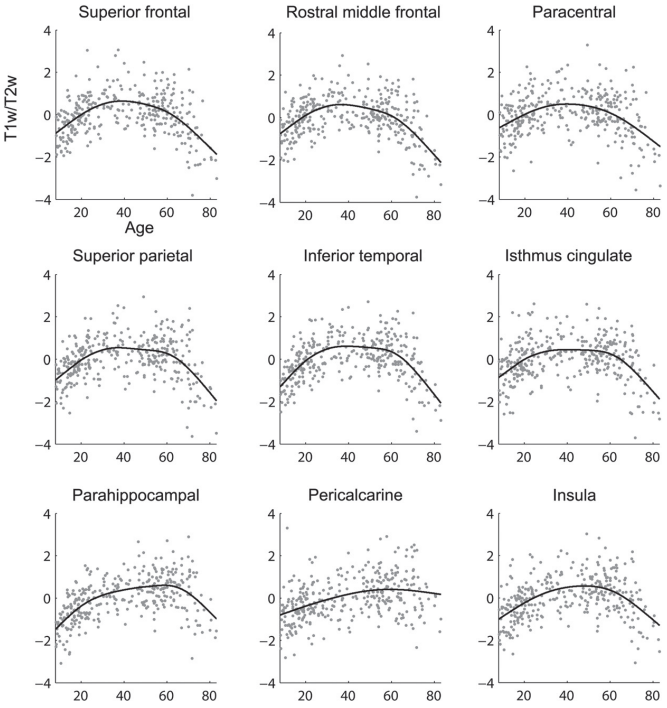

Figure 6. Lifespan WM T1w/T2w ratio trajectories in the subjacent WM to the selected cortical ROIs. Values are standardized residual after regression of the T2w matrix; please see Materials and Methods for details. Age values are in years.

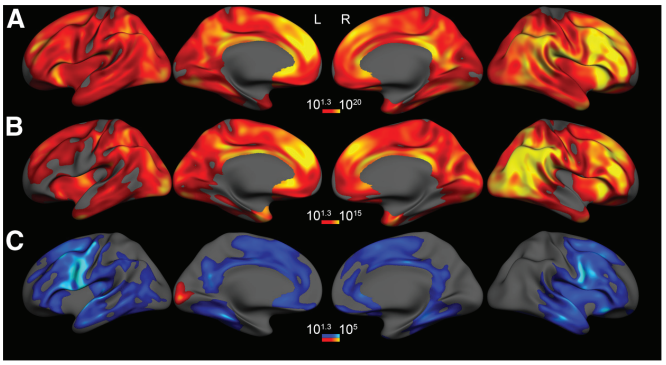

Figure 7. DTI-derived MD and age. *p*-value maps showing the relationship between MD and the quadratic effects of age in all subjects (age 8–83 years; ***A***), the quadratic effects of age in the adult subsample (age 20–83 years; ***B***), and the linear effects of age in the young subsample (age 8–19 years; ***C***), respectively. The effects are corrected for multiple comparisons, but actual *p*-values are shown. See Table 2 for clusterwise *p*-values.

When including WM T1w/T2w as a per-vertex regressor to assess the specificity of the GM T1w/T2w-IIV association, the effects were reduced to a cluster of 2880 vertices (1.8%) with peak in the superior temporal cortex in the adults. No interaction effect of age and IIV on GM T1w/T2w remained when controlling for WM T1w/T2w. For the youngest subsample, the inclusion of WM T1w/T2w did not alter the results (four clusters in the left hemisphere covering 23.6% of the vertices with peaks in superior parietal, supramarginal, and pre- and paracentral cortices, respectively, and 16.3% of the vertices in the right hemisphere peaking in superior parietal, postcentral, and insula showed a positive relationship between sdRT and T1w/T2w ratio).

We repeated the above analyses assessing functional correlates of intracortical myelin, now testing for a relationship between IIV and intracortical MD separately for the adult and young subsample (Fig. 10*A*). One left hemisphere cluster covering 3% of the vertices peaking in the pericalcarine cortex and extending dorsally into precuneus and posterior cingulate cortices showed a

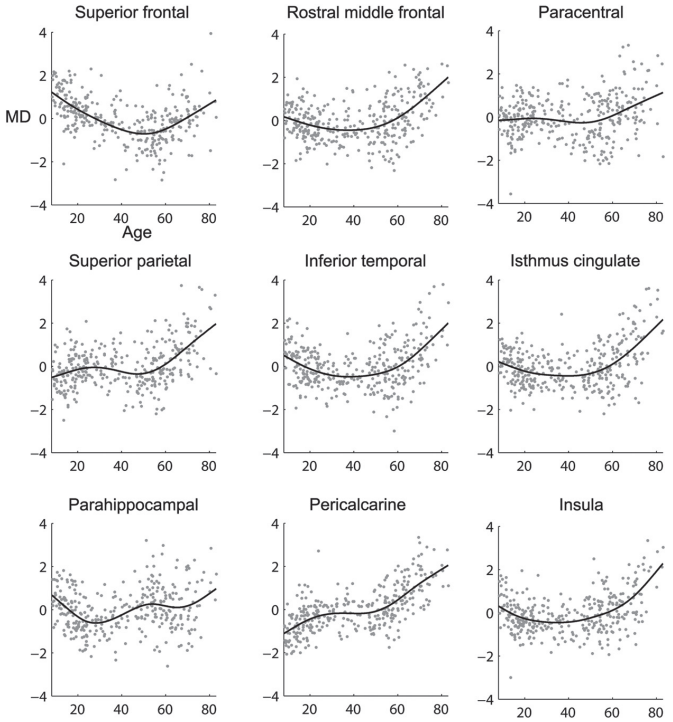

Figure 8. Lifespan MD trajectories in selected cortical ROIs. MD values are standardized *z*-scores. Age values are in years.

positive relationship between sdRT and MD in the adults. In the right hemisphere, 2 clusters with peaks in pars triangularis and lingual cortices, respectively, covering a total of 5% of the surface showed a similar positive relationship. Therefore, increased variability in task performance was related to higher MD. Again, the relationships were relatively modest, with mean correlations of 0.21 and 0.26 in the left and right significant clusters, respectively. In the young subsample (Fig. 10*B*), 1 cluster covering 5% of the vertices with peak value in the left precentral cortex extending anteriorly, showed a positive relationship between MD and sdRT, as previously observed in the adult subsample. A similar cluster was found in the right hemisphere in addition to a superior frontal cluster (each 2% of all vertices). Two clusters peaking in the left and right pericalcarine cortex (1% of the vertices, respectively) showed a negative relationship, indicating that increased variability in task performance was related to lower MD in this occipital region. In addition, a right mainly lateral occipital cluster, but with peak value in posterior middle temporal cortex, also showed a similar negative relationship (1% of the vertices). The relationships were stronger, mean positive correlations were 0.43 and 0.42, and mean negative correlations were −0.38 and −0.32, for left and right hemispheres, respectively.

To investigate whether the relation between MD and sdRT changes as a function of age, we added the interaction term age × sdRT to the previous linear model including age and sex as global variables and thickness as a per-vertex variable. As seen in Figure 10*C*, in the adults, 1 left hemisphere cluster of 7035 vertices (4.3%) peaking in the posterior cingulate cortex but extending anteriorly through the entire cingulate cortex and medial superior frontal cortices showed significant positive age interactions, indicating a stronger relationship between MD and IIV with increasing age (mean $r = 0.06$ in the youngest half of the sample and 0.14 in the oldest half). A similar pattern was seen in the right hemisphere, however, the effects were much more widespread, with six clusters covering 48,031 vertices (29.3%) peaking in the rostral middle frontal, precentral, precuneus, inferior parietal, entorhinal, and lingual cortices. Again, the positive relationship between MD and IIV manifests itself mainly in the oldest group, as can be seen in the scatter plots, in which the adult group has been divided by the median age into two groups; mean correlations were 0.02 and 0.12 in the oldest half for the left and right hemispheres, respectively, and −0.05 and −0.10 in the youngest half of the adult sample (<52 years).

As for the T1w/T2w-IIV analyses, we reran the regression analyses after excluding studentized deleted residuals exceeding ±2.5, including FIQ as a covariate to assess specificity. Again, all MD and IIV associations remained highly significant and FIQ did not yield a unique statistical contribution on MD. The IIV-MD associations generally did not change. For the adults, the IIV-MD association increased slightly in left (Pearson's *r* from 0.21 to 0.26; 6 cases exceeding the threshold of 2.5) and right hemispheres (from 0.26 to 0.31; 4 cases exceeding the threshold). The age-IIV interaction correlations with MD were reduced for the youngest adults in the left (from −0.05 to −0.02; 3 cases exceeding the threshold) and right hemispheres (from −0.10 to −0.05; 5 cases exceeding the threshold). For the oldest adults, the left hemisphere correlations increased slightly (from 0.02 to 0.05), and a slight decrease was found in the right hemisphere (from 0.12 to 0.10). In the youngest subsample, the positive correlations were slightly increased in the left hemisphere (from 0.43 to 0.46; 1 case exceeding the threshold) and reduced in the right hemisphere (from 0.42 to 0.38; 2 case exceeding the threshold). The negative correlations increased in both left (from −0.38 to −0.41; 1 case exceeding the threshold) and right hemispheres (from −0.32 to −0.38; 2 case exceeding the threshold).

Discussion

Although methodological advances in neuroimaging have ignited great interest in macrostructural properties of the cerebral cortex and microstructural properties of WM throughout life, intracortical lifespan changes have mainly eluded close examination. This is in contrast to the fact that the unfolding of cortical myelination and demyelination from birth to senium has interested neuroscientists for more than a century (Kaes, 1907). Here, using a myelin-mapping approach (Glasser and Van Essen, 2011), we characterized the degree of intracortical myelin in 339 subjects 8–83 years of age. We found inverse U-shaped lifespan trajectories across the cortex, with substantial heterogeneity across different regions. Association cortices tended to show the most curved trajectories, indicating protracted intracortical myelin development and vulnerability to aging. Similar effects

were seen for DTI-derived MD. Myelin content correlated with within-subject variability on a speeded performance task signaling behavioral correlates of individual differences in cortical myelin. The results suggest that myelin mapping *in vivo* detects effects of age on intracortical myelin grade in development and aging and, importantly, is associated with cognition. Therefore, mapping myelin by use of T1w/T2w MRI could be a valuable neuroscientific tool for studying effects on intracortical myelin content across various populations and conditions.

Lifespan changes in intracortical myelination

The location and extent of important cortical areas characterized using high-resolution T1w images in marmosets and T1w/T2w ratio maps in humans agree closely in direct and indirect comparisons, respectively, with myelin histology (Bock et al., 2011; Glasser and Van Essen, 2011). Although additional validation is required, these findings provide support of the interpretation of T1w/T2w ratio as an estimate of myelin. Our T1w/T2w ratio myelin maps generally demonstrate inverted U-shaped trajectories, indicating a three-staged process of cortical myelin changes: an accelerated myelination process until ~30 years of age, followed by a period of relative stability, before a decrease in myelin content from the late 50s. DTI-derived MD, partly influenced by myelin (Beaulieu, 2002), mapped from the same vertices as the T1w/T2w ratio generally showed U-shaped patterns, although demonstrating less maturational effects in some regions. All findings were statistically independent of concurrent cortical thinning. The results accord with the seminal histology study by Yakovlev and Lecours (1967), who reported an increase of myelinated fibers in the association cortices until the third decade and possibly beyond. However, discrepancies with lifespan histology studies of restricted regions exist (Lintl and Braak, 1983; Benes et al., 1994). For example, Benes (1989) reported stable myelination of the cingulate cortices from the second decade. However, the relative sparsity of data points in lower or upper age ranges in these studies limits conclusions regarding lifespan trajectories. Studies using a combination of histology and imaging would be particularly informative in untangling these findings and in further substantiating the link between T1w/T2w ratio and myelin.

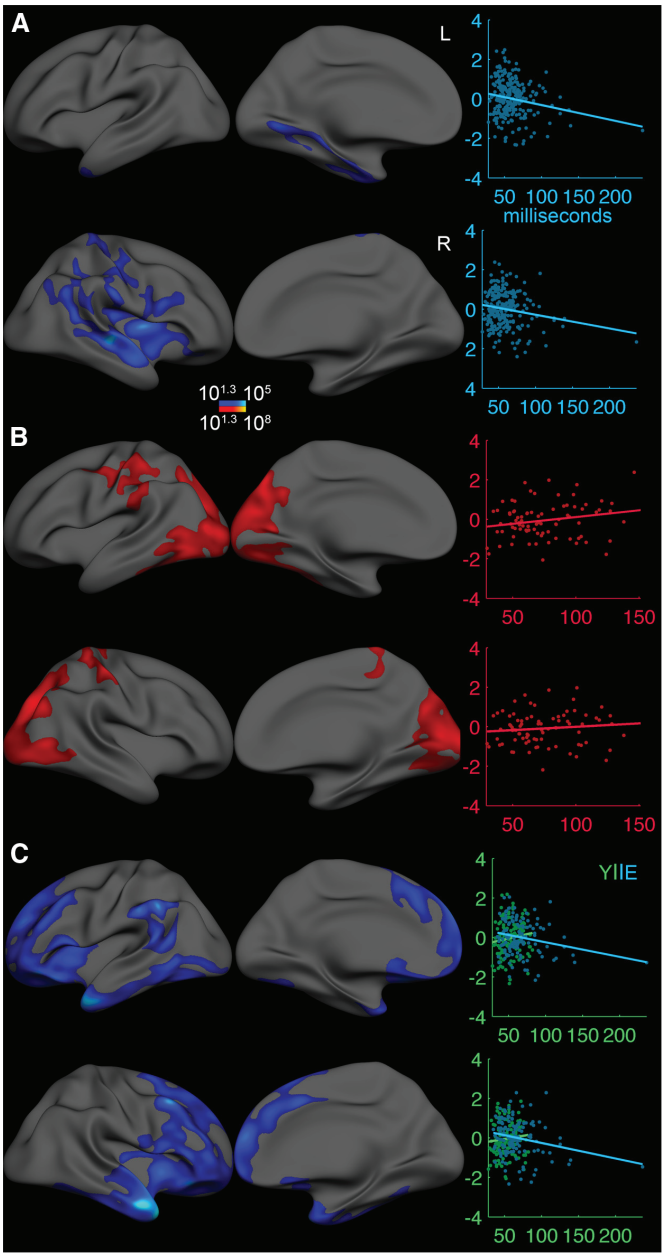

Figure 9. The relationship between T1w/T2w ratio and IIV. Left, *p*-values maps showing the relationship between T1w/T2w ratio and IIV in the adults (***A***), the young (***B***), and the interaction between age and IIV in adults (***C***). The effects are corrected for multiple comparisons, but actual *p*-values are shown. See Table 2 for clusterwise *p*-values. Right, Scatterplots illustrating the surface-based analyses; values are *z*-values of mean residuals after excluding studentized deleted residuals exceeding ±2 and regressing T1w/T2w on sex, age, T2w matrix, mRT, FIQ, and thickness (please see Materials and Methods for details). Y, young adults (<52 years); E, elderly (≥52 years).

The T1w/T2w ratio approach refines our efforts using T1w intensity to trace cortical changes in an overlapping sample (Westlye et al., 2010b). As in the present study, a three-phasic function was delineated, with the greatest age-related decrease observed from the late 50s. However, peaks were estimated to be earlier; for example, the superior parietal cortex peaked in the

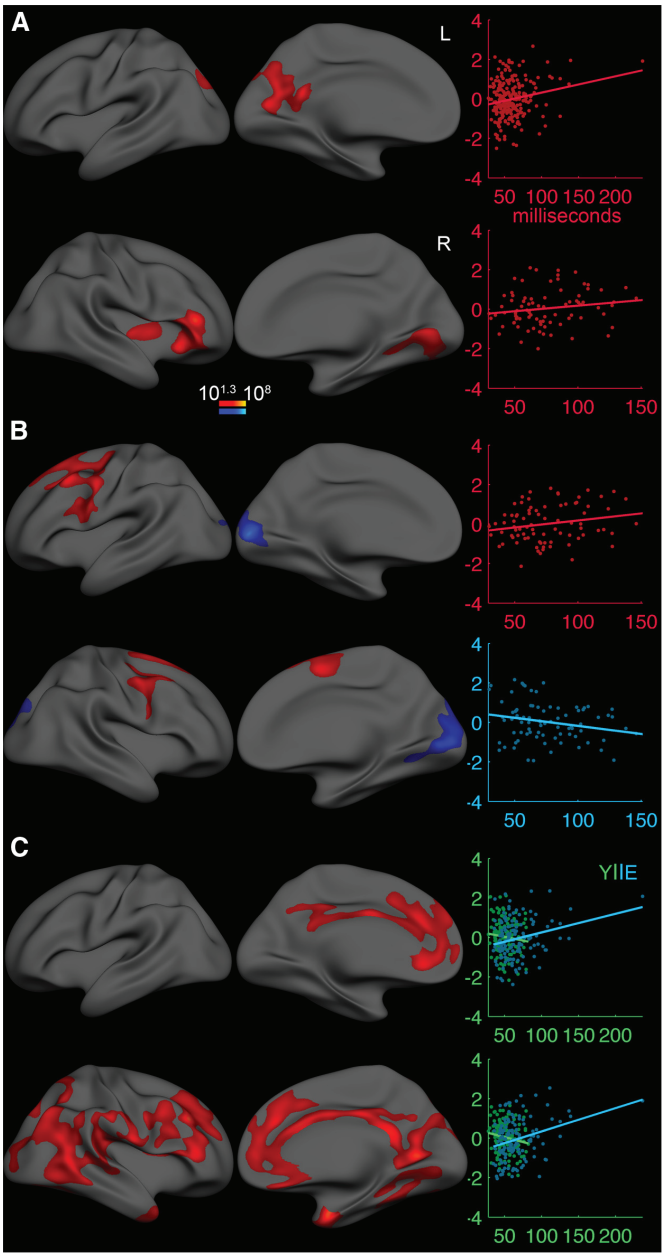

Figure 10. Relationship between MD and IIV. Left, *P*-values maps showing the relationship between T1w/T2w ratio and IIV in the adults (***A***), the young (***B***), and the interaction between age and IIV in adults (***C***). The effects are corrected for multiple comparisons, but actual *p*-values are shown. See Table 2 for clusterwise *p*-values. Right, Scatterplots illustrating the surface-based analyses; values are *z*-values of mean residuals after excluding studentized deleted residuals exceeding ±2 and regressing MD on sex, age, mRT, FIQ, and thickness (see Materials and Methods for details). Please note that in ***B***, scatterplots are only shown for the positive cluster in the left hemisphere and for the negative cluster in the right hemisphere. Y, young adults (<52 years); E, elderly (≥52 years).

middle of the second decade of life. In addition to minor processing differences, Westlye et al. (2010b) normalized the T1w signal at each voxel by CSF signal intensity. The local normalization by the corresponding voxel in the T2w image might render the T1w/T2w method more accurate. However, although the bias field in the T1w and T2w sequences are highly correlated, they are not identical (Glasser et al., 2013), which may favor the use of only T1w intensity either normalized by CSF or as a GM/WM ratio (Westlye et al., 2009b). Longitudinal imaging studies using a multimodal approach will help to settle the observed disagreements.

Cognitive correlates

IIV reflects performance fluctuations during a single task session (Stuss et al., 2003) and is increased in, for example, attention deficit hyperactivity disorder and mild dementia (Hultsch et al., 2000; Castellanos and Tannock, 2002). We recently related greater IIV to widespread WM integrity reductions (Fjell et al., 2011; Tamnes et al., 2012). Here, we link IIV to degree of myelin within cortical regions. The effects were independent of general intellectual abilities and were right lateralized, which is consistent with a greater specialization of the right cortices for visuospatial attention (Mesulam, 1981; Corbetta et al., 1993). The findings concur with correlations between aging-related myelin defects in the prefrontal cortex and cognitive impairment in primates (Peters and Sethares, 2002). In humans, Blackmon et al. (2011) used a ratio of GM and WM T1w intensity and found left-lateralized correlations with verbal working memory performance. Here, we extend this finding by associating cognitive functioning specifically to cortical myelin content. A potential mechanism relates reduced myelin to decreased structural and functional connectivity (Garrett et al., 2011), increasing neural noise (MacDonald et al., 2009). We have previously reported cortical thickness–attention correlations in an overlapping sample (Westlye et al., 2011), effects possibly influenced by myelin changes. Although speeded tasks constitute a prime candidate for studying cognition–myelin relationships, future studies should assess how cortical myelin might have implications for other aspects of cognition, especially in aging (Salthouse, 1996).

As expected based on our previous WM studies, the relationship between IIV and intracortical microstructure was strongest in the elderly (≥52 years). The results suggest that the weakest relationship between IIV and microstructure manifest in groups of participants showing less variance in microstructural properties and IIV, whereas a relationship appeared in elderly participants, in whom individual differences may be

larger. However, the mechanisms underlying age-related alterations on myelin remain poorly understood. A host of processes disrupting myelin have been reported in aging primates, for example, increased thickness of myelin sheaths (Peters et al., 2001) and formation of myelin balloons (Feldman and Peters, 1998). It is likely that these changes differ compared with the myelination occurring during development (Tau and Peterson, 2010). Such possible differential effects during development and aging may have different cognitive correlates. Moreover, we mainly observed that increased intracortical myelin (higher T1w/T2w ratio or lower MD) related to less variable performance. This relationship is consistent with our hypothesis based on the beneficial effects of myelin for neural conduction (Zalc and Colman, 2000). However, the opposite relationship was found in the young subsample covering posterior regions. The effects could relate to greater maturational compared with aging-related changes (Tamnes et al., 2013), increasing the age term in our model and thereby reducing residual variance. Although complex relations between structure and function exist in development (Shaw et al., 2006), the current data do not allow us to rule out regional maturational effects of myelin beyond improving conduction velocity and timing (Fields, 2008).

The adult IIV-T1w/T2w associations mostly disappeared when accounting for WM myelin levels. This suggests concurrent WM and GM axonal aging processes with similar behavior correlates (Peters and Kemper, 2012), but awaits exploration in clinical conditions (Grydeland et al., 2010). The WM curves, generally in accordance with previous WM DTI findings (Westlye et al., 2010a; Lebel et al., 2012), showed a somewhat less protracted development compared with GM. Both curves generally evidenced decline from the late 50s, but were more pronounced in WM. We expected relatively similar age effects (Westlye et al., 2010a, 2010b) and the slight discrepancies in age associations might stem from greater amount of myelin in WM and increased WM/GM boundary blurring with age (Salat et al., 2009), probably with a larger impact on GM values, potentially rendering the WM age trajectories more accurate.

Limitations and future directions of research

Although T1w and T2w images largely reflect myelin (Eickhoff et al., 2005), cell density and iron (Fukunaga et al., 2010) likely contribute. Future studies will benefit from high-resolution scans. Thin and heavily myelinated areas such as the pericalcarine cortex may suffer more from partial-volume effects (Glasser and Van Essen, 2011), potentially yielding incorrect T1w/T2w ratio and MD values. The decrease in pericalcarine cortical thickness through the lifespan (Westlye et al., 2009b) may exacerbate the effects with age and cause the lack of decrease in myelin with age observed here. Similarly, the 2 mm isotropic resolution of the DTI images causes partial-volume of tissue types when assessing thin cortices. In addition, these cross-sectional findings should be confirmed by longitudinal change measurements.

Conclusion

We mapped intracortical myelin through the lifespan using T1/T2w MRI intensities and generally observed a three-phasic relationship in which myelin increased until ~30 years of age and remained relatively stable before a decline started around the end of the 50s. A relationship between intracortical myelin and intrasession performance variability was observed in widespread regions. This link was strongest with increasing age, suggesting that aging-related intracortical myelin changes contribute to increased IIV. Corresponding findings were generally observed for MD sampled from the same vertices. The results suggest that myelin mapping by MRI constitute a viable method for studying intracortical myelin differences and cognition in development and aging. The relatively short scan times and conventional protocols also hold hope for potential application in aiding detection (Grydeland et al., 2013) in clinical populations, including dementia (Bosch et al., 2012), schizophrenia (Alexander-Bloch et al., 2013), and multiple sclerosis (Hulst and Geurts, 2011).

References

Abe O, Yamasue H, Aoki S, Suga M, Yamada H, Kasai K, Masutani Y, Kato N, Kato N, Ohtomo K (2008) Aging in the CNS: comparison of gray/white matter volume and diffusion tensor data. Neurobiol Aging 29:102–116. CrossRef Medline

Alexander-Bloch AF, Vértes PE, Stidd R, Lalonde F, Clasen L, Rapoport J, Giedd J, Bullmore ET, Gogtay N (2013) The anatomical distance of functional connections predicts brain network topology in health and schizophrenia. Cereb Cortex 23:127–138. CrossRef Medline

Bartzokis G (2004) Age-related myelin breakdown: a developmental model of cognitive decline and Alzheimer's disease. Neurobiol Aging 25:5–18; author reply 49–62. Medline

Bartzokis G, Beckson M, Lu PH, Nuechterlein KH, Edwards N, Mintz J (2001) Age-related changes in frontal and temporal lobe volumes in men: a magnetic resonance imaging study. Arch Gen Psychiatr 58:461–465. Medline

Beaulieu C (2002) The basis of anisotropic water diffusion in the nervous system–a technical review. NMR Biomed 15:435–455. CrossRef Medline

Beck AT, Steer R (1987) Beck depression inventory scoring manual. New York: The Psychological Corporation.

Benes FM (1989) Myelination of cortical-hippocampal relays during late adolescence. Schizophr Bull 15:585–593. CrossRef Medline

Benes FM, Turtle M, Khan Y, Farol P (1994) Myelination of a key relay zone in the hippocampal formation occurs in the human brain during childhood, adolescence, and adulthood. Arch Gen Psychiatr 51:477–484. Medline

Blackmon K, Halgren E, Barr WB, Carlson C, Devinsky O, DuBois J, Quinn BT, French J, Kuzniecky R, Thesen T (2011) Individual differences in verbal abilities associated with regional blurring of the left gray and white matter boundary. J Neurosci 31:15257–15263. CrossRef Medline

Bock NA, Hashim E, Kocharyan A, Silva AC (2011) Visualizing myeloarchitecture with magnetic resonance imaging in primates. Ann N Y Acad Sci 1225(suppl 1):E171–E181. CrossRef Medline

Bosch B, Arenaza-Urquijo EM, Rami L, Sala-Llonch R, Junqué C, Solé-Padullés C, Peña-Gómez C, Bargalló N, Molinuevo JL, Bartrés-Faz D (2012) Multiple DTI index analysis in normal aging, amnestic MCI and AD. Relationship with neuropsychological performance. Neurobiol Aging 33:61–74. CrossRef Medline

Carreiras M, Seghier ML, Baquero S, Estévez A, Lozano A, Devlin JT, Price CJ (2009) An anatomical signature for literacy. Nature 461:983–986. CrossRef Medline

Castellanos FX, Tannock R (2002) Neuroscience of attention-deficit/hyperactivity disorder: the search for endophenotypes. Nat Rev Neurosci 3:617–628. CrossRef Medline

Concha L, Gross DW, Wheatley BM, Beaulieu C (2006) Diffusion tensor imaging of time-dependent axonal and myelin degradation after corpus callosotomy in epilepsy patients. Neuroimage 32:1090–1099. CrossRef Medline

Corbetta M, Miezin FM, Shulman GL, Petersen SE (1993) A PET study of visuospatial attention. J Neurosci 13:1202–1226. Medline

Dale AM, Fischl B, Sereno MI (1999) Cortical surface-based analysis. I. Segmentation and surface reconstruction. Neuroimage 9:179–194. CrossRef Medline

Debener S, Ullsperger M, Siegel M, Fiehler K, von Cramon DY, Engel AK (2005) Trial-by-trial coupling of concurrent electroencephalogram and functional magnetic resonance imaging identifies the dynamics of performance monitoring. J Neurosci 25:11730–11737. CrossRef Medline

Desikan RS, Ségonne F, Fischl B, Quinn BT, Dickerson BC, Blacker D, Buckner RL, Dale AM, Maguire RP, Hyman BT, Albert MS, Killiany RJ (2006) An automated labeling system for subdividing the human cerebral cortex on MRI scans into gyral based regions of interest. Neuroimage 31:968–980. CrossRef Medline

Eickhoff S, Walters NB, Schleicher A, Kril J, Egan GF, Zilles K, Watson JD, Amunts K (2005) High-resolution MRI reflects myeloarchitecture and cytoarchitecture of human cerebral cortex. Hum Brain Mapp 24:206–215. CrossRef Medline

Eriksen BA, Eriksen CW (1974) Effects of noise letters upon the identification of a target letter in a nonsearch task. Perception & Psychophysics 16:143–149. CrossRef

Feldman ML, Peters A (1998) Ballooning of myelin sheaths in normally aged macaques. J Neurocytol 27:605–614. CrossRef Medline

Fields RD (2008) White matter in learning, cognition and psychiatric disorders. Trends Neurosci 31:361–370. CrossRef Medline

Fischl B, Dale AM (2000) Measuring the thickness of the human cerebral cortex from magnetic resonance images. Proc Natl Acad Sci U S A 97:11050–11055. CrossRef Medline

Fischl B, Sereno MI, Dale AM (1999a) Cortical surface-based analysis. II: Inflation, flattening, and a surface-based coordinate system. Neuroimage 9:195–207. CrossRef Medline

Fischl B, Sereno MI, Tootell RB, Dale AM (1999b) High-resolution intersubject averaging and a coordinate system for the cortical surface. Hum Brain Mapp 8:272–284. CrossRef Medline

Fischl B, Salat DH, Busa E, Albert M, Dieterich M, Haselgrove C, van der Kouwe A, Killiany R, Kennedy D, Klaveness S, Montillo A, Makris N, Rosen B, Dale AM (2002) Whole brain segmentation: automated labeling of neuroanatomical structures in the human brain. Neuron 33:341–355. CrossRef Medline

Fischl B, Salat DH, van der Kouwe AJ, Makris N, Ségonne F, Quinn BT, Dale AM (2004a) Sequence-independent segmentation of magnetic resonance images. Neuroimage 23(suppl 1):S69–S84.

Fischl B, van der Kouwe A, Destrieux C, Halgren E, Ségonne F, Salat DH, Busa E, Seidman LJ, Goldstein J, Kennedy D, Caviness V, Makris N, Rosen B, Dale AM (2004b) Automatically parcellating the human cerebral cortex. Cereb Cortex 14:11–22. CrossRef Medline

Fjell AM, Westlye LT, Amlien I, Espeseth T, Reinvang I, Raz N, Agartz I, Salat DH, Greve DN, Fischl B, Dale AM, Walhovd KB (2009) High consistency of regional cortical thinning in aging across multiple samples. Cereb Cortex 19:2001–2012. CrossRef Medline

Fjell AM, Walhovd KB, Westlye LT, Østby Y, Tamnes CK, Jernigan TL, Gamst A, Dale AM (2010) When does brain aging accelerate? Dangers of quadratic fits in cross-sectional studies. Neuroimage 50:1376–1383. CrossRef Medline

Fjell AM, Westlye LT, Amlien IK, Walhovd KB (2011) Reduced white matter integrity is related to cognitive instability. J Neurosci 31:18060–18072. CrossRef Medline

Folstein MF, Folstein SE, McHugh PR (1975) "Mini-mental state". A practical method for grading the cognitive state of patients for the clinician. J Psychiatr Res 12:189–198. CrossRef Medline

Fukunaga M, Li TQ, van Gelderen P, de Zwart JA, Shmueli K, Yao B, Lee J, Maric D, Aronova MA, Zhang G, Leapman RD, Schenck JF, Merkle H, Duyn JH (2010) Layer-specific variation of iron content in cerebral cortex as a source of MRI contrast. Proc Natl Acad Sci U S A 107:3834–3839. CrossRef Medline

Garrett DD, Kovacevic N, McIntosh AR, Grady CL (2011) The importance of being variable. J Neurosci 31:4496–4503. CrossRef Medline

Glasser MF, Van Essen DC (2011) Mapping human cortical areas in vivo based on myelin content as revealed by T1- and T2-weighted MRI. J Neurosci 31:11597–11616. CrossRef Medline

Glasser MF, Goyal MS, Preuss TM, Raichle ME, Van Essen DC (2013) Trends and properties of human cerebral cortex: correlations with cortical myelin content. Neuroimage. Advance online publication. doi: 10.1016/j.neuroimage.2013.03.060. CrossRef Medline

Gogtay N, Giedd JN, Lusk L, Hayashi KM, Greenstein D, Vaituzis AC, Nugent TF 3rd, Herman DH, Clasen LS, Toga AW, Rapoport JL, Thompson PM (2004) Dynamic mapping of human cortical development during childhood through early adulthood. Proc Natl Acad Sci U S A 101:8174–8179. CrossRef Medline

Greve DN, Fischl B (2009) Accurate and robust brain image alignment using boundary-based registration. Neuroimage 48:63–72. CrossRef Medline

Grydeland H, Walhovd KB, Westlye LT, Due-Tønnessen P, Ormaasen V, Sundseth Ø, Fjell AM (2010) Amnesia following herpes simplex encephalitis: diffusion-tensor imaging uncovers reduced integrity of normal-appearing white matter. Radiology 257:774–781. CrossRef Medline

Grydeland H, Westlye LT, Walhovd KB, Fjell AM (2013) Improved prediction of Alzheimer's disease with longitudinal white matter/gray matter contrast changes. Hum Brain Mapp 34:2775–2785. CrossRef Medline

Hagler DJ Jr, Saygin AP, Sereno MI (2006) Smoothing and cluster thresholding for cortical surface-based group analysis of fMRI data. Neuroimage 33:1093–1103. CrossRef Medline

Hulst HE, Geurts JJ (2011) Gray matter imaging in multiple sclerosis: what have we learned? BMC Neurol 11:153. CrossRef Medline

Hultsch DF, MacDonald SW, Hunter MA, Levy-Bencheton J, Strauss E (2000) Intraindividual variability in cognitive performance in older adults: comparison of adults with mild dementia, adults with arthritis, and healthy adults. Neuropsychology 14:588–598. CrossRef Medline

Jenkinson M, Smith S (2001) A global optimisation method for robust affine registration of brain images. Med Image Anal 5:143–156. CrossRef Medline

Kaes T (1907) Die Grosshirnrinde des Menschen in ihren Massen und in ihrem Fasergehalt. Jena: Fischer.

Kochunov P, Glahn DC, Lancaster J, Thompson PM, Kochunov V, Rogers B, Fox P, Blangero J, Williamson DE (2011) Fractional anisotropy of cerebral white matter and thickness of cortical gray matter across the lifespan. Neuroimage 58:41–49. CrossRef Medline

Koo BB, Hua N, Choi CH, Ronen I, Lee JM, Kim DS (2009) A framework to analyze partial volume effect on gray matter mean diffusivity measurements. Neuroimage 44:136–144. CrossRef Medline

Lebel C, Beaulieu C (2011) Longitudinal development of human brain wiring continues from childhood into adulthood. J Neurosci 31:10937–10947. CrossRef Medline

Lebel C, Gee M, Camicioli R, Wieler M, Martin W, Beaulieu C (2012) Diffusion tensor imaging of white matter tract evolution over the lifespan. Neuroimage 60:340–352. CrossRef Medline

Lintl P, Braak H (1983) Loss of intracortical myelinated fibers: a distinctive age-related alteration in the human striate area. Acta Neuropathol 61:178–182. CrossRef Medline

MacDonald SW, Li SC, Bäckman L (2009) Neural underpinnings of within-person variability in cognitive functioning. Psychol Aging 24:792–808. CrossRef Medline

Mesulam MM (1981) A cortical network for directed attention and unilateral neglect. Ann Neurol 10:309–325. CrossRef Medline

Nieuwenhuys R (2013) The myeloarchitectonic studies on the human cerebral cortex of the Vogt-Vogt school, and their significance for the interpretation of functional neuroimaging data. Brain Struct Funct 218:303–352. CrossRef Medline

Panizzon MS, Fennema-Notestine C, Kubarych TS, Chen CH, Eyler LT, Fischl B, Franz CE, Grant MD, Hamza S, Jak A, Jernigan TL, Lyons MJ, Neale MC, Prom-Wormley EC, Seidman L, Tsuang MT, Wu H, Xian H, Dale AM, Kremen WS (2012) Genetic and environmental influences of white and gray matter signal contrast: a new phenotype for imaging genetics? Neuroimage 60:1686–1695. CrossRef Medline

Paus T (2005) Mapping brain maturation and cognitive development during adolescence. Trends Cogn Sci 9:60–68. CrossRef Medline

Peters A, Kemper T (2012) A review of the structural alterations in the cerebral hemispheres of the aging rhesus monkey. Neurobiol Aging 33:2357–2372. CrossRef Medline

Peters A, Sethares C (2002) Aging and the myelinated fibers in prefrontal cortex and corpus callosum of the monkey. J Comp Neurol 442:277–291. CrossRef Medline

Peters A, Sethares C, Killiany RJ (2001) Effects of age on the thickness of myelin sheaths in monkey primary visual cortex. J Comp Neurol 435:241–248. CrossRef Medline

Pierpaoli C, Jezzard P, Basser PJ, Barnett A, Di Chiro G (1996) Diffusion tensor MR imaging of the human brain. Radiology 201:637–648. Medline

Reese TG, Heid O, Weisskoff RM, Wedeen VJ (2003) Reduction of eddy-current-induced distortion in diffusion MRI using a twice-refocused spin echo. Magn Reson Med 49:177–182. CrossRef Medline

Salat DH, Lee SY, van der Kouwe AJ, Greve DN, Fischl B, Rosas HD (2009) Age-associated alterations in cortical gray and white matter signal intensity and gray to white matter contrast. Neuroimage 48:21–28. CrossRef Medline

Salthouse TA (1996) The processing-speed theory of adult age differences in cognition. Psychol Rev 103:403–428. CrossRef Medline

Ségonne F, Dale AM, Busa E, Glessner M, Salat D, Hahn HK, Fischl B (2004)

A hybrid approach to the skull stripping problem in MRI. Neuroimage 22:1060–1075. CrossRef Medline

Shaw P, Greenstein D, Lerch J, Clasen L, Lenroot R, Gogtay N, Evans A, Rapoport J, Giedd J (2006) Intellectual ability and cortical development in children and adolescents. Nature 440:676–679. CrossRef Medline

Sigalovsky IS, Fischl B, Melcher JR (2006) Mapping an intrinsic MR property of gray matter in auditory cortex of living humans: a possible marker for primary cortex and hemispheric differences. Neuroimage 32:1524–1537. CrossRef Medline

Sled JG, Zijdenbos AP, Evans AC (1998) A nonparametric method for automatic correction of intensity nonuniformity in MRI data. IEEE Trans Med Imaging 17:87–97. CrossRef Medline

Smith SM (2002) Fast robust automated brain extraction. Hum Brain Mapp 17:143–155. CrossRef Medline

Smith SM, Jenkinson M, Woolrich MW, Beckmann CF, Behrens TE, Johansen-Berg H, Bannister PR, De Luca M, Drobnjak I, Flitney DE, Niazy RK, Saunders J, Vickers J, Zhang Y, De Stefano N, Brady JM, Matthews PM (2004) Advances in functional and structural MR image analysis and implementation as FSL. Neuroimage 23(suppl 1):S208–S219. CrossRef Medline

Song SK, Sun SW, Ramsbottom MJ, Chang C, Russell J, Cross AH (2002) Dysmyelination revealed through MRI as increased radial (but unchanged axial) diffusion of water. Neuroimage 17:1429–1436. CrossRef Medline

Song SK, Yoshino J, Le TQ, Lin SJ, Sun SW, Cross AH, Armstrong RC (2005) Demyelination increases radial diffusivity in corpus callosum of mouse brain. Neuroimage 26:132–140. CrossRef Medline

Sowell ER, Peterson BS, Thompson PM, Welcome SE, Henkenius AL, Toga AW (2003) Mapping cortical change across the human life span. Nat Neurosci 6:309–315. CrossRef Medline

Stuss DT, Murphy KJ, Binns MA, Alexander MP (2003) Staying on the job: the frontal lobes control individual performance variability. Brain 126:2363–2380. CrossRef Medline

Tamnes CK, Østby Y, Fjell AM, Westlye LT, Due-Tønnessen P, Walhovd KB (2010) Brain maturation in adolescence and young adulthood: regional age-related changes in cortical thickness and white matter volume and microstructure. Cereb Cortex 20:534–548. CrossRef Medline

Tamnes CK, Fjell AM, Westlye LT, Østby Y, Walhovd KB (2012) Becoming consistent: developmental reductions in intraindividual variability in reaction time are related to white matter integrity. J Neurosci 32:972–982. CrossRef Medline

Tamnes CK, Walhovd KB, Dale AM, Østby Y, Grydeland H, Richardson G, Westlye LT, Roddey JC, Hagler DJ Jr, Due-Tønnessen P, Holland D, Fjell AM (2013) Brain development and aging: overlapping and unique patterns of change. Neuroimage 68:63–74. CrossRef Medline

Tau GZ, Peterson BS (2010) Normal development of brain circuits. Neuropsychopharmacology 35:147–168. CrossRef Medline

Vogt O (1910) The myeloarchitectonic tesselated mosaicism of the human front-brain. J für Psychologie und Neurologie 15:221–232.

Wechsler D (1999) Wechsler abbreviated scale of intelligence. San Antonio, TX: The Psychological Corporation.

Westlye LT, Walhovd KB, Bjørnerud A, Due-Tønnessen P, Fjell AM (2009a) Error-related negativity is mediated by fractional anisotropy in the posterior cingulate gyrus–a study combining diffusion tensor imaging and electrophysiology in healthy adults. Cereb Cortex 19:293–304. CrossRef Medline

Westlye LT, Walhovd KB, Dale AM, Espeseth T, Reinvang I, Raz N, Agartz I, Greve DN, Fischl B, Fjell AM (2009b) Increased sensitivity to effects of normal aging and Alzheimer's disease on cortical thickness by adjustment for local variability in gray/white contrast: a multi-sample MRI study. Neuroimage 47:1545–1557. CrossRef Medline

Westlye LT, Walhovd KB, Dale AM, Bjørnerud A, Due-Tønnessen P, Engvig A, Grydeland H, Tamnes CK, Østby Y, Fjell AM (2010a) Life-span changes of the human brain white matter: diffusion tensor imaging (DTI) and volumetry. Cereb Cortex 20:2055–2068. CrossRef Medline

Westlye LT, Walhovd KB, Dale AM, Bjørnerud A, Due-Tønnessen P, Engvig A, Grydeland H, Tamnes CK, Østby Y, Fjell AM (2010b) Differentiating maturational and aging-related changes of the cerebral cortex by use of thickness and signal intensity. Neuroimage 52:172–185. CrossRef Medline

Westlye LT, Grydeland H, Walhovd KB, Fjell AM (2011) Associations between regional cortical thickness and attentional networks as measured by the attention network test. Cereb Cortex 21:345–356. CrossRef Medline

Woolrich MW, Jbabdi S, Patenaude B, Chappell M, Makni S, Behrens T, Beckmann C, Jenkinson M, Smith SM (2009) Bayesian analysis of neuroimaging data in FSL. Neuroimage 45:S173–186. CrossRef Medline

Yakovlev PI, Lecours A-R (1967) The myelogenic cycles of regional maturation of the brain. In: Regional development of the brain in early life (Minkowski A, ed), pp 3–70. Oxford and Edinburg: Blackwell Scientific Publications.

Yoshiura T, Higano S, Rubio A, Shrier DA, Kwok WE, Iwanaga S, Numaguchi Y (2000) Heschl and superior temporal gyri: low signal intensity of the cortex on T2-weighted MR images of the normal brain. Radiology 214:217–221. Medline

Zalc B, Colman DR (2000) Origins of vertebrate success. Science 288:271–272. Medline